The C-terminal RRM/ACT domain is crucial for fine-tuning the activation of 'long' RelA-SpoT Homolog enzymes by ribosomal complexes

Hiraku Takada[1,2,*], Mohammad Roghanian[1,2], Victoriia Murina[1,2], Ievgen Dzhygyr[1,2], Rikinori Murayama[3], Genki Akanuma[4], Gemma C. Atkinson[1], Abel Garcia-Pino[5,6], Vasili Hauryliuk[1,2,7*]

[1]Department of Molecular Biology, Umeå University, Umeå, Sweden

[2]Laboratory for Molecular Infection Medicine Sweden (MIMS), Umeå University, Umeå, Sweden

[3]Akita Prefectural Research Center for Public Health and Environment, 6-6 Senshu-Kubotamachi, Akita, 010-0874, Japan

[4]Department of Life Science, Graduate School of Science, Gakushuin University, Tokyo, Japan

[5]Cellular and Molecular Microbiology, Faculté des Sciences, Université Libre de Bruxelles (ULB), Building BC, Room 1C4 203, Boulevard du Triomphe, 1050, Brussels, Belgium

[6]WELBIO, Avenue Hippocrate 75, 1200 Brussels, Belgium

[7]University of Tartu, Institute of Technology, 50411 Tartu, Estonia

*** Correspondence:**
Hiraku Takada
hiraku.takada@umu.se
Vasili Hauryliuk
vasili.hauryliuk@umu.se

Keywords: ppGpp[1], Rel[2], ACT[3], RRM[4], stringent response[5], ribosome[6]

Running title: Rel/RelA regulation by the RRM/ACT domain

Abstract: The (p)ppGpp-mediated stringent response is a bacterial stress response implicated in virulence and antibiotic tolerance. Both synthesis and degradation of the (p)ppGpp alarmone nucleotide are mediated by RelA-SpoT Homolog (RSH) enzymes which can be broadly divided in two classes: single-domain 'short' and multi-domain 'long' RSH. The regulatory ACT (Aspartokinase, Chorismate mutase and TyrA) / RRM (RNA Recognition Motif) domain is a near-universal C-terminal domain of long RSHs. Deletion of RRM in both monofunctional (synthesis-only) RelA as well as bifunctional (i.e. capable of both degrading and synthesising the alarmone) Rel renders the long RSH cytotoxic due to overproduction of (p)ppGpp. To probe the molecular mechanism underlying this effect we characterised *Escherichia coli* RelA and *Bacillus subtilis* Rel RSHs lacking RRM. We demonstrate that, first, the cytotoxicity caused by the removal of RRM is counteracted by secondary mutations that disrupt the interaction of the RSH with the starved ribosomal complex – the ultimate inducer of (p)ppGpp production by RelA and Rel – and, second, that the hydrolytic activity of Rel is not abrogated in the truncated mutant. Therefore, we conclude that the overproduction of (p)ppGpp by RSHs lacking the RRM domain is not explained by a lack of auto-inhibition in the absence of RRM or/and a defect in (p)ppGpp hydrolysis. Instead, we argue that it is driven by misregulation of the RSH activation by the ribosome.

1 Introduction

Bacteria employ diverse mechanisms to sense and respond to stress. One such mechanism is the stringent response – a near-universal stress response orchestrated by hyper-phosphorylated derivatives of housekeeping nucleotides GDP and GTP: guanosine tetraphosphate (ppGpp) and guanosine pentaphosphate (pppGpp), collectively referred to as (p)ppGpp (Hauryliuk et al., 2015;Liu et al., 2015;Steinchen and Bange, 2016). Since the stringent response and (p)ppGpp-mediated signalling are implicated in virulence, antibiotic resistance and tolerance (Dalebroux et al., 2010;Dalebroux and Swanson, 2012;Hauryliuk et al., 2015), this stress signalling system has been recently targeted for development of new anti-infective compounds (Kushwaha et al., 2019).

Both synthesis and degradation of (p)ppGpp is mediated by RelA/SpoT Homolog (RSH) enzymes. RSHs can be broadly divided into two classes: 'long' multi-domain and 'short' single-domain factors (Atkinson et al., 2011;Jimmy et al., 2019). In the majority of bacteria, including model Gram-positive bacterial species *Bacillus subtilis*, the long multi-domain RSHs are represented by one bifunctional enzyme, Rel (Mittenhuber, 2001;Atkinson et al., 2011). Beta- and Gammaproteobacteria, such as *Escherichia coli*, encode two long RSH factors – RelA and SpoT – which are the products of gene duplication and diversification of the ancestral *rel* stringent factor (Mittenhuber, 2001;Atkinson et al., 2011;Hauryliuk et al., 2015). *E. coli* RelA is the most well-studied long RSH. RelA is a dedicated sensor of amino acid starvation with strong (p)ppGpp synthesis activity that is induced by ribosomal complexes harbouring cognate deacylated tRNA in the A-site, so-called 'starved' ribosomal complexes (Haseltine and Block, 1973). Unlike RelA, which lacks (p)ppGpp hydrolysis activity (Shyp et al., 2012), Rel and SpoT can both synthesise and degrade (p)ppGpp (Xiao et al., 1991;Avarbock et al., 2000). Similarly to RelA – and to the exclusion of SpoT – (p)ppGpp synthesis by Rel is strongly activated by starved ribosomes (Avarbock et al., 2000). In addition to long RSHs, bacteria often encode single domain RSH enzymes: Small Alarmone Synthetases (SAS) and Small Alarmone Hydrolases (SAH) (Atkinson et al., 2011;Jimmy et al., 2019), such as RelQ and RelP in the Firmicute bacterium *B. subtilis* (Nanamiya et al., 2008).

Long RSHs are universally comprised of two functional regions: the catalytic N-terminal domains (NTD) and the regulatory C-terminal domains (CTD) (**Figure 1A**) (Atkinson et al., 2011). The NTD region comprises the (p)ppGpp hydrolase domain (HD; enzymatically inactive in RelA) and the (p)ppGpp synthetase domain (SYNTH) linked by an α-helical region that regulates the allosteric crosstalk between both domains (Tamman et al., 2019). The CTD encompasses four domains: the Thr-tRNA synthetase, GTPase and SpoT domain (TGS), the Helical domain, the Zing Finger Domain (ZFD) (equivalent to Ribosome-InterSubunit domain, RIS, as per (Loveland et al., 2016), or Conserved Cysteine, CC, as per (Atkinson et al., 2011)), and, finally, the RNA Recognition Motif domain (RRM) (equivalent to Aspartokinase, Chorismate mutase and TyrA, ACT, as per (Atkinson et al., 2011)). When Rel/RelA is bound to a starved ribosomal complex, the TGS domain inspects the deacylated tRNA in the A-site and the TGS domain interacts directly with the 3' CCA end of the A-site tRNA (Arenz et al., 2016;Brown et al., 2016;Loveland et al., 2016). The conserved histidine 432 residue of *E. coli* RelA mediating this interaction is crucial for activation of RelA's enzymatic activity by the 3' CCA (Winther et al., 2018). Both ZFD and RRM interact with the A-site finger (ASF) of the 23S ribosomal RNA (Arenz et al., 2016;Brown et al., 2016;Loveland et al., 2016), and in *E. coli* RelA this contact is crucial for efficient recruitment to and activation by starved ribosomal complexes (Kudrin et al., 2018).

While the NTD is responsible for the enzymatic function of RSHs, the CTD senses the starved ribosomal complex and transmits the signal to activate NTD-mediated (p)ppGpp synthesis by Rel/RelA

84 (Agirrezabala et al., 2013;Arenz et al., 2016;Brown et al., 2016;Loveland et al., 2016). Since removal
85 of the CTD increases the rate of (p)ppGpp production by Rel/RelA in the absence of ribosomes or
86 starved complexes, the CTD was proposed to mediate the auto-inhibition of the NTD synthetase
87 activity, thus precluding uncontrolled production of cytotoxic (p)ppGpp (Schreiber et al., 1991;Gropp
88 et al., 2001;Mechold et al., 2002;Avarbock et al., 2005;Jiang et al., 2007;Yang et al., 2019).

89 The specific focus of this study is the C-terminal RRM/ACT domain of ribosome-associated RSH RelA
90 and Rel. The RRM is absent in RelA enzymes from *Methylotenera mobilitas,*
91 *Elusimicrobium minutum*, *Francisella philomiraga* and *Francisella tularensis* (Atkinson et al., 2011).
92 The only experimentally characterised representative amongst these is *F. tularensis* RelA (Wilkinson
93 et al., 2015). In a reconstituted biochemical system, the factor behaves similarly to *E. coli* RelA, i.e. it
94 has very low synthesis activity by itself and is potently activated by the ribosome. Conversely, deletion
95 of the RRM domain in factors that naturally possess it leads to inhibition of growth (Gratani et al.,
96 2018;Ronneau et al., 2019;Turnbull et al., 2019) that is mediated by over-production of (p)ppGpp in
97 the cell, as shown for *Caulobacter crescentus* Rel (Ronneau et al., 2019) and *E. coli* RelA (Turnbull et
98 al., 2019). The exact molecular mechanism of misregulation remains unclear. Deletion of RRM in
99 bifunctional *C. crescentus* Rel leads to compromised hydrolase activity (Ronneau et al., 2019), while
100 overproduction of (p)ppGpp by monofunctional *E. coli* RelA$^{\Delta RRM}$ was suggested to be due to
101 upregulated constitutive synthesis activity, conceivably due to defective auto-inhibition of the NTD
102 synthetase domain by the CTD (Turnbull et al., 2019).

103 In this report, we inspected the possible role of the ribosome in overproduction of (p)ppGpp by ΔRRM
104 variants of long RSHs in the cell. By characterising versions of *E. coli* RelA and *B. subtilis* Rel, we
105 demonstrate that the cytotoxicity of mutant RSH variants is strictly dependent on the interaction with
106 the ribosome and deacylated tRNA, and, therefore, cannot be explained by defects in intra-molecular
107 regulation alone.

108 2 Materials and Methods

109 2.1 Multiple sequence alignment

110 Sequences were aligned with MAFFT v7.164b with the L-ins-i strategy (Katoh and Standley, 2013),
111 and alignments were visualised with Jalview (Waterhouse et al., 2009).

112 2.2 Construction of bacterial strains and plasmids

113 The strains and plasmids used in this study are listed in **Supplementary Tables 1-3**. Oligonucleotides
114 used in this study are provided in **Supplementary Table 4**. A detailed description of strain construction
115 is provided in the *Supplementary Material*.

116 2.3 Growth assays

117 *E. coli* BW25113 cells were transformed with expression constructs either based on a high-copy IPTG
118 inducible vector pUC derivative pMG25 (pMG25::*relA* (Turnbull et al., 2019), pNDM220::*relA*$^{\Delta RRM}$,
119 pNDM220::*spoR* or pNDM220::*spoT*$^{\Delta RRM}$) or on a low-copy IPTG inducible vector, mini R1 plasmid
120 pNDM220 which is present in one to two copies per chromosome (Molin et al., 1979)
121 (pNDM220::*relA*, pNDM220::*relA*$^{\Delta RRM}$, pNDM220::*relA*$^{\Delta RRM\text{-}H432E}$, pNDM220::*relA*$^{\Delta RRM\text{-}R629E}$ or
122 pNDM220::*relA*$^{\Delta RRM\text{-}C612A/C613A}$). For solid medium growth assays, ten-fold serial dilutions of overnight
123 LB cultures were spotted onto LB agar supplemented with 30 µg/mL ampicillin and 1 mM IPTG. For
124 liquid medium growth assays, thousand-fold dilutions of the overnight LB cultures were made in liquid

125 LB supplemented with 30 μg/mL ampicillin and 1 mM IPTG, seeded on a 100-well honeycomb plate
126 (Oy Growth Curves AB Ltd, Helsinki, Finland), and plates incubated in a Bioscreen C (Labsystems,
127 Helsinki, Finland) at 37 °C with continuous medium shaking.

128 *B. subtilis* strains were pre-grown on LB plates lacking the IPTG inducer overnight (10 hours) at 30 °C.
129 Fresh individual colonies were used to inoculate filtered LB medium in the presence of indicated
130 concentrations of IPTG and OD_{600} adjusted to 0.01. The cultures were seeded on a 100-well
131 honeycomb plate (Oy Growth Curves AB Ltd, Helsinki, Finland), and plates were incubated in a
132 Bioscreen C (Labsystems, Helsinki, Finland) at 37 °C with continuous medium shaking.

133 Growth rates (μ_2) were calculated as slopes of linear regression lines through $\log_2$-transformed OD_{600}
134 data points.

135 **2.4 Preparation of polyclonal anti-Rel antiserum**

136 The entire coding region of the *B. subtilis rel* gene was amplified by PCR using the synthetic
137 oligonucleotide pQErelA_F and pQErelA_R containing a BamHI site and *B. subtilis* genomic DNA as
138 a template. The resulting PCR fragment was cut with BamHI and then inserted into the BamHI sites of
139 pQE60 (Qiagen), yielding plasmid pQErelA. pOErelA was transformed into *E. coli* M15 (pREP4)
140 (Qiagen), fresh transformants were inoculated into LB liquid culture (1000 mL) with 100 μg/mL
141 ampicillin and grown at 37 °C with vigorous shaking. At OD_{600} of 0.8 expression of Rel induced with
142 1 mM IPTG (final concentration). After 3 hours of expression the cells were harvested by
143 centrifugation, resuspended in buffer A (500 mM NaCl, 50 mM Tris-HCl pH 8.0) supplemented with
144 2 mM PMSF and lysed by sonication. Rel-His_6 inclusion bodies were collected by centrifugation,
145 resuspended in buffer A supplemented with 8 M guanidine hydrochloride (= buffer B) and loaded onto
146 an Ni-NTA agarose column (QIAGEN) pre-equilibrated in the same buffer. The column was washed
147 with buffer B supplemented with 10 mM imidazole, and the protein was eluted with a 100-400 mM
148 imidazole gradient in buffer B. The fractions containing Rel-His_6 was dialyzed against buffer A at 4 °C
149 overnight. Aggregated Rel-His_6 protein was collected by centrifugation, resuspended in buffer A
150 supplemented with 6 M urea and used for rabbit immunization. Rabbit serum was used as a polyclonal
151 anti-Rel antibody.

152 **2.5 Sucrose gradient fractionation and Western blotting**

153 *B. subtilis* strains were pre-grown on LB plates overnight at 30 °C. Fresh individual colonies were used
154 to inoculate 200 mL LB cultures that were grown at 37 °C. At OD_{600} of 0.2 amino acid starvation was
155 induced by addition of isoleucyl tRNA synthetase inhibitor mupirocin (dissolved in DMSO,
156 AppliChem) to final concentration of 700 nM for 20 minutes. As a mock control, a separate culture
157 was treated with the same amount of DMSO. After 20 minutes the cells were collected by
158 centrifugation (8,000 rpm, 5 minutes, JLA-16.25 Beckman Coulter rotor), dissolved in 0.5 mL of
159 HEPES:Polymix buffer (5 mM $Mg(OAc)_2$) supplemented with 2 mM PMSF, lysed using FastPrep
160 homogenizer (MP Biomedicals) by four 20 seconds pulses at speed 6.0 mp/sec with chilling on ice for
161 1 minutes between the cycles), and clarified by ultracentrifugation (14,800 rpm for 20 minutes,
162 Microfuge 22R centrifuge Beckman Coulter, F241.5P rotor). Clarified cell lysates were loaded onto
163 10-35% sucrose gradients in HEPES:Polymix buffer pH 7.5 (5 mM Mg^{2+} final concentration),
164 subjected to centrifugation (36,000 rpm for 3 hours at 4 °C, SW-41Ti Beckman Coulter rotor) and
165 analysed using Biocomp Gradient Station (BioComp Instruments) with A_{260} as a readout.

166 For Western blotting 0.5 mL fractions were supplemented with 1.5 mL of 99.5% ethanol, precipitated
167 overnight at –20 °C. After centrifugation at 14,800 rpm for 30 minutes at 4 °C the supernatants were

168 discarded and the samples were dried. The pellets were resuspended in 40 µL of 2xSDS loading buffer
169 (100 mM Tris-HCl pH 6.8, 4% SDS (w/v) 0.02% Bromophenol blue, 20% glycerol (w/v) 4% β-
170 mercaptoethanol), resolved on the 8% SDS PAGE and transferred to nitrocellulose membrane (Trans-
171 Blot Turbo Midi Nitrocellulose Transfer Pack, Bio-Rad , 0.2 µm pore size) with the use of a Trans-
172 Blot Turbo Transfer Starter System (Bio-Rad) (10 minutes, 2.5A, 25V). Membrane blocking was done
173 for one hour in PBS-T (1xPBS 0.05% Tween-20) with 5% w/v nonfat dry milk at room temperature.
174 Rel was detected using anti-Rel primary combined with goat anti-rabbit IgG-HRP secondary
175 antibodies. All antibodies were used at 1:10,000 dilution. ECL detection was performed using
176 WesternBright™ Quantum (K-12042-D10, Advansta) Western blotting substrate and an ImageQuant
177 LAS 4000 (GE Healthcare) imaging system.

178 **2.6 Expression and purification of *E. coli* RelA and *B. subtilis* Rel**

179 Wild type and H432E mutant variants of *E. coli* RelA were expressed and purified as described earlier
180 (Turnbull et al., 2019).

181 Wild type and mutant variants of *B. subtilis* Rel were overexpressed in freshly transformed *E. coli*
182 BL21 DE3 Rosetta (Novagen). Fresh transformants were inoculated to final OD_{600} of 0.05 in the LB
183 medium (800 mL) supplemented with 100 µg/mL kanamycin. The cultures were grown at 37 °C until
184 an OD_{600} of 0.5, induced with 1 mM IPTG (final concentration) and grown for additional 1.5 hour at
185 30 °C. The cells were harvested by centrifugation and resuspended in buffer A (750 mM KCl, 5 mM
186 $MgCl_2$, 40 µM $MnCl_2$, 40 µM $Zn(OAc)_2$, 1 mM mellitic acid (Tokyo Kasei Kogyo Co., Ltd.), 20 mM
187 imidazole, 10% glycerol, 4 mM β-mercaptoethanol, 25 mM HEPES:KOH pH 8) supplemented with
188 0.1 mM PMSF and 1 U/mL of DNase I. Cells were lysed by one passage through a high-pressure cell
189 disrupter (Stansted Fluid Power, 150 MPa), cell debris was removed by centrifugation (25,000 rpm for
190 40 min, JA-25.50 Beckman Coulter rotor) and clarified lysate was taken for protein purification.

191 To prevent possible substitution of Zn^{2+} ions in Rel's Zn-finger domain for Ni^{2+} during purification on
192 an Ni-NTA metal affinity chromatography column (Block et al., 2009), a 5 mL HisTrap HP column
193 was stripped from Ni^{2+} in accordance with manufacturer's recommendations, washed with 5 column
194 volumes (CV) of 100 mM $Zn(OAc)_2$ pH 5.0 followed by 5 CV of deionized water. Clarified cell lysate
195 was filtered through a 0.2 µm syringe filter and loaded onto the Zn^{2+}-charged HisTrap 5 mL HP column
196 pre-equilibrated in buffer A. The column was washed with 5 CV of buffer A, and the protein was eluted
197 with a linear gradient (6 CV, 0-100% buffer B) of buffer B (750 mM KCl, 5 mM $MgCl_2$, 40 µM $MnCl_2$,
198 40 µM $Zn(OAc)_2$, 1 mM mellitic acid, 500 mM imidazole, 10% glycerol, 4 mM β-mercaptoethanol,
199 25 mM HEPES:KOH pH 8). Mellitic acid forms highly ordered molecular networks when dissolved
200 in water (Inabe, 2005) and it was shown to promote the stability of *Thermus thermophilus* Rel (Van
201 Nerom et al., 2019). Fractions most enriched in Rel (≈25-50% buffer B) were pooled, totalling
202 approximately 5 mL. The sample was loaded on a HiLoad 16/600 Superdex 200 pg column pre-
203 equilibrated with a high salt buffer (buffer C; 2 M NaCl, 5 mM $MgCl_2$, 10% glycerol, 4 mM β-
204 mercaptoethanol, 25 mM HEPES:KOH pH 8). The fractions containing Rel were pooled and applied
205 on HiPrep 10/26 desalting column (GE Healthcare) pre-equilibrated with storage buffer (buffer D; 720
206 mM KCl, 5 mM $MgCl_2$, 50 mM arginine, 50 mM glutamic acid, 10% glycerol, 4 mM β-
207 mercaptoethanol, 25 mM HEPES:KOH pH 8). Arginine and glutamic acid were added to improve
208 protein solubility and long-term stability (Golovanov et al., 2004). The fractions containing Rel were
209 collected and concentrated in an Amicon Ultra (Millipore) centrifugal filter device (cut-off 50 kDa).
210 To cleave off the His_{10}-SUMO tag, 35 µg of His_6-Ulp1 per 1 mg of Rel were added and the reaction
211 mixture was incubated at room temperature for 15 min. After the His_{10}-SUMO tag was cleaved off, the
212 protein was passed though 5 mL Zn^{2+}-charged HisTrap HP pre-equilibrated with buffer D. Fractions

213 containing Rel in the flow-through were collected and concentrated on Amicon Ultra (Millipore)
214 centrifugal filter device with 50 kDa cut-off. The purity of protein preparations was assessed by SDS-
215 PAGE and spectrophotometrically (OD_{260}/OD_{280} ratio below 0.8 corresponding to less than 5% RNA
216 contamination (Layne, 1957)). Protein preparations were aliquoted, frozen in liquid nitrogen and stored
217 at –80 °C. Individual single-use aliquots were discarded after the experiment.

218 **2.7 Negative staining electron microscopy**

219 3.5 µL of 2 µM Rel protein was loaded onto a glow-discharged Cu_{300} grid (TAAB Laboratories
220 Equipment Ltd.) with manually layered 2.9 nm carbon. The sample was incubated on the grid for 1-3
221 minutes, blotted with Watman filter paper, than twice washed with water and blotted, stained with
222 1.5% uranyl acetate pH 4.2 for 30 seconds before the final blotting. Grids were dried on the bench and
223 imaged by Talos L 120C (FEI) microscope with 92,000X magnification.

224 **2.8 Preparation of 10X Polymix buffer base**

225 The 10X Polymix base was prepared as per (Antoun et al., 2004), with minor modifications. For
226 preparation of the putrescine solution, 100 g of putrescine (1,4-diaminobutane) was dissolved in 600
227 mL of ddH_2O at 90 °C, and the pH adjusted with acetic acid to 8.0 (approximately 100 mL of 100%
228 acetic acid). After cooling to room temperature, the pH was adjusted further to 7.6 and the volume was
229 adjusted to the final of 2 L by addition of 1.134 L of ddH_2O. One 100 mL cup of activated charcoal
230 was added and the slurry was stirred under the hood for 30 minutes. The slurry was filtered through,
231 first, Whatman paper and then through a 0.45 µm BA85 membrane. The final solution was stored at
232 4 °C in a bottle wrapped in foil since putrescine is photosensitive. The preparation of 2 L of 10X
233 Polymix buffer base used 141.66 g KCl, 5.35 g NH_4Cl, 21.44 g $Mg(OAc)_2 \bullet 4H_2O$, 1.47 g $CaCl_2 \bullet 2H_2O$,
234 5.092 g spermidine, and 160 ml of putrescine solution (described above). The salts were dissolved in
235 ddH_2O (≈1,500 mL), then the putrescine solution was added and mixed well. Spermidine was dissolved
236 in a small volume of ddH_2O and added to the mixture. The pH was adjusted to 7.5 with concentrated
237 acetic acid or 5 M KOH, and after that the volume was adjusted by adding ddH_2O to 2 L. The buffer
238 was filtered through 0.2 µm nitrocellulose filter (2-3 filters are needed). The resulting 10X Polymix
239 buffer base was aliquoted and stored at –20 °C. The final working HEPES:Polymix buffer was made
240 using the 10X Polymix buffer base, 1M DDT and 1 M HEPES:KOH pH 7.5 and contains 20 mM
241 HEPES:KOH pH 7.5, 2 mM DTT, 5 mM $MgOAc_2$, 95 mM KCl, 5 mM NH_4Cl, 0.5 mM $CaCl_2$, 8 mM
242 putrescine, 1 mM spermidine.

243 **2.9 Purification of *B. subtilis* 70S ribosomes**

244 *B. subtilis* strain RIK2508 (*trpC2* Δ*hpf*) strain (Akanuma et al., 2016;Brodiazhenko et al., 2018) was
245 pre-grown on LB plates overnight at 30 °C. Fresh individual colonies were used to inoculate LB liquid
246 cultures (25 × 400 mL) to OD_{600} of 0.05 and grown at 37 °C with vigorous shaking. At OD_{600} 1.2 the
247 cells were pelleted at 4 °C (TLA10.500 (Beckman), 15 min at 5,000-8,000 rcf), resuspended with ice-
248 cold PBS buffer, pelleted again in 50 mL Falcon tubes, frozen with liquid nitrogen and stored at –80
249 °C. Approximately 20 g of frozen *B. subtilis* cells were resuspended in 50 mL of cell opening buffer
250 (100 mM NH_4Cl, 15 mM $Mg(OAc)_2$, 0.5 mM EDTA, 3 mM β-mercaptoethanol, 20 mM Tris:HCl pH
251 7.5) supplemented with 1 mU Turbo DNase (Thermo Fisher Scientific), 0.1 mM PMSF and 35 µg/mL
252 lysozyme, incubated on ice for one hour, and opened by three passages on a high-pressure cell disrupter
253 (Stansted Fluid Power) at 220 MPa. Lysed cells were clarified by centrifugation for 40 min at 40,000
254 rpm (Ti 45 rotor, Beckman), NH_4Cl concentration was adjusted to 400 mM, and the mixture was
255 filtered through 0.45 µm syringe filters. The filtrated lysate was loaded onto a pre-equilibrated 80 mL
256 CIMmultus QA-80 column (BIA Separations, quaternary amine advanced composite column) at a flow

rate of 20 mL/min, and the column washed with 5 CV (CV = 80 mL) of low salt buffer (400 mM NH_4Cl, 15 mM $Mg(OAc)_2$, 3 mM β-mercaptoethanol, 20 mM Tris:HCl pH 7.5). Ribosomes were then eluted in 45 mL fractions by a step gradient to 77% high salt buffer (900 mM NH_4Cl, 15 mM $Mg(OAc)_2$, 3 mM β-mercaptoethanol, 20 mM Tris:HCl pH 7.5) for 5 CV, followed by 100% high salt buffer for 1 CV. The fractions containing ribosomes were pooled, the concentration of NH_4Cl was adjusted to 100 mM, and the ribosomes were treated with puromycin added to a final concentration of 10 μM. The resultant crude 70S preparation was resolved on a 10-40% sucrose gradient in overlay buffer (60 mM NH_4Cl, 15 mM $Mg(OAc)_2$, 0.25 mM EDTA, 3 mM β-mercaptoethanol, 20 mM Tris:HCl pH 7.5) in a zonal rotor (Ti 15, Beckman, 17 hours at 21,000 rpm). The peak containing pure 70S ribosomes was pelleted by centrifugation (20 hours at 35,000 rpm), and the final ribosomal preparation was dissolved in HEPES:Polymix buffer (20 mM HEPES:KOH pH 7.5, 2 mM DTT, 5 mM $Mg(OAc)_2$, 95 mM KCl, 5 mM NH_4Cl, 0.5 mM $CaCl_2$, 8 mM putrescine, 1 mM spermidine (Antoun et al., 2004)). 70S concentration was measured spectrophotometrically (1 OD_{260} corresponds to 23 nM of 70S) and ribosomes were aliquoted (50-100 μL per aliquot), snap-frozen in liquid nitrogen and stored at –80 °C.

2.10 Preparation of 70S initiation complexes (70S IC)

Initiation complexes were prepared by as per (Murina et al., 2018), with minor modifications. The reaction mix containing *B. subtilis* 70S ribosomes (final concentration of 6 μM) with *E. coli* IF1 (4 μM), IF2 (5 μM), IF3 (4 μM), ^{3}H-fMet-tRNA$_i^{fMet}$ (8 μM), mRNA MVFStop (8 μM, 5'-GGC**AAGGAGGA**GAUAAGA<u>AUGGUUUUCUAA</u>UA-3'; Shine-Dalgarno sequence is highlighted in bold, ORF is underlined), 1 mM GTP and 2 mM DTT in 1×HEPES:Polymix buffer (20 mM HEPES:KOH pH 7.5, 95 mM KCl, 5 mM NH_4Cl, 5 mM $Mg(OAc)_2$, 0.5 mM $CaCl_2$, 8 mM putrescine, 1 mM spermidine, 1 mM DTT (Antoun et al., 2004)) was incubated at 37 °C for 30 min. Then the ribosomes were pelleted through a sucrose cushion (1.1 M sucrose in HEPES:Polymix buffer with 15 mM Mg^{2+}) at 50,000 rpm for two hours (TLS-55, Beckman), the pellet was dissolved in HEPES:Polymix buffer (5 mM $Mg(OAc)_2$), aliquoted, frozen in liquid nitrogen and stored at –80 °C.

2.11 Preparation of ^{3}H-labelled pppGpp

3 μM *E. fecalis* RelQ (Beljantseva et al., 2017) were incubated in reaction buffer (18 mM $MgCl_2$, 20 mM DTT, 20 M Tris-HCl pH 8.0) together with 8 mM ATP and 5 mM ^{3}H-GTP (SA: 100 cpm/pmol) for 2 hours at 37 °C to produce ^{3}H-pppGpp. The resultant mixture was loaded on strong anion-exchange column (MonoQ 5/50 GL; GE Healthcare), and nucleotides were resolved by a 0.5-1,000 mM LiCl gradient. Peak fractions containing ^{3}H-pppGpp were pooled and precipitated by addition of lithium chloride to a final concentration of 1 M followed by addition of four volumes of ethanol. The suspension was incubated at –80 °C overnight and centrifuged (14,800 rpm, 30 min, 4 °C). The resulting pellets were washed with absolute ethanol, dried, dissolved in 20 mM HEPES-KOH buffer (pH 7.5) and stored at –80 °C.

2.12 ^{3}H-pppGpp hydrolysis assay

The reaction mixtures contained 140-250 nM Rel, 300 μM ^{3}H-pppGpp, 1 mM $MnCl_2$, an essential cofactor for Rel's hydrolysis activity (Avarbock et al., 2000;Mechold et al., 2002;Tamman et al., 2019), all in HEPES:Polymix buffer (5 mM Mg^{2+} final concentration). After preincubation at 37 °C for 3 minutes, the reaction was started by the addition of prewarmed Rel and 5 μL aliquots were taken throughout the time course of the reaction and quenched with 4 μL 70% formic acid supplemented with a cold nucleotide standard (4 mM GTP) for UV-shadowing.

300 **2.13 ^{3}H-pppGpp synthesis assay**

301 Assays with *E. coli* RelA were performed as described earlier (Kudrin et al., 2018). In the case of
302 *B. subtilis* Rel, the reaction mixtures typically contained 500 nM *B. subtilis* 70S IC(MVF), 140 nM
303 Rel, guanosine nucleoside substrate (300 μM ^{3}H-GTP, PerkinElmer), 100 μM pppGpp, 2 μM *E. coli*
304 tRNA^{Val} (Chemical Block), all in HEPES:Polymix buffer (5 mM Mg^{2+} final concentration). After
305 preincubation at 37 °C for 3 minutes, the reaction was started by the addition of prewarmed ATP to
306 the final concentration of 1 mM, and 5 μL aliquots were taken throughout the time course of the
307 reaction and quenched with 4 μL 70% formic acid supplemented with a cold nucleotide standard (4
308 mM GTP) for UV-shadowing. Individual quenched timepoints were spotted PEI-TLC plates
309 (Macherey-Nagel) and nucleotides were resolved in 1.5 KH_2PO_4 pH 3.5 buffer. The TLC plates were
310 dried, cut into sections as guided by UV-shadowing, and ^{3}H radioactivity was quantified by scintillation
311 counting in EcoLite™ Liquid Scintillation Cocktail (MP Biomedicals).

312 **3 Results**

313 **3.1 Toxicity of *E. coli* ΔRRM RelA is countered by mutations compromising the interaction**
314 **with starved ribosomes**

315 As we have shown earlier, low-level ectopic expression of RelA$^{\Delta RRM}$ from a low copy number
316 pNDM220 plasmid under the control of a $P_{A1/O4/O3}$ promoter has a more pronounced inhibitory effect
317 on *E. coli* growth in comparison with expression of the full-length protein (Turnbull et al., 2019). We
318 tested whether $P_{A1/O4/O3}$-driven high-level expression of RelA$^{\Delta RRM}$ from a high-copy pUC derivative
319 pMG25 would cause a more pronounced growth defect (**Figure 2A**). For comparison, we tested the
320 effects of expression of the second *E. coli* RSH enzyme – SpoT – using both the full-length and the
321 ΔRRM variants. Even in the absence of the IPTG inducer, leaky expression of RelA$^{\Delta RRM}$ has a dramatic
322 effect on *E. coli* growth, while the full-length protein does not have an effect. In the presence of 50 μM
323 IPTG, both full-length and RelA$^{\Delta RRM}$ inhibit the growth, although the latter has a stronger effect;
324 induction with 500 μM IPTG completely abrogates the growth in both cases. While expression of SpoT
325 has a detectable inhibitory effect at 500 μM IPTG, the effect is the same for full-length and SpoT$^{\Delta RRM}$.
326 Since even leaky expression of RelA$^{\Delta RRM}$ inhibits growth, we concluded that this high-level expression
327 system is ill-suited for follow-up microbiological investigations. Therefore, to test whether the toxicity
328 of RelA$^{\Delta RRM}$ in *E. coli* is dependent on the interaction with starved complexes, we used the pNDM220-
329 based low-level expression system used previously (Turnbull et al., 2019). Guided by the recent cryo-
330 EM reconstructions of RelA (Arenz et al., 2016;Brown et al., 2016;Loveland et al., 2016), we designed
331 a set of mutations that will specifically disrupt RelA's interaction with starved ribosomal complexes.

332 To disrupt the interaction between RelA and the tRNA, we adopted the H432E mutation in the TGS
333 domain that was earlier shown to specifically abrogate the recognition of the 3' CCA end of the A/R
334 tRNA (Winther et al., 2018). This conserved histidine residue stacks between the two cytosine bases
335 and hydrogen-bonds the phosphodiester backbone (**Figure 1B**). Replacing it with glutamic acid
336 introduces a charge repulsion effect as well as a steric clash. To disrupt the interaction with the
337 ribosome we used mutations in the ZFD: R629E as well as a double substitution C602A C603A; both
338 mutants are expected to compromise the recognition of the 23S rRNA ASF element that is crucial for
339 RelA recruitment (Kudrin et al., 2018). The conserved double motif docks the ZFD α-helix into the
340 major groove of the ASF; replacement by alanine is expected to abrogate this interaction (**Figure 1C**).
341 The conserved arginine 629 residue is in close proximity to A886-A887 and A885-A886
342 phosphodiester bonds (3.5Å and 5Å, respectively), and, therefore, the R629E substitution is expected
343 to cause electrostatic repulsion.

344 Low-level expression of full-length RelA has a minor, but detectable growth inhibitory effect both
345 when tested on solid LB agar media (**Figure 2B**) and in liquid LB cultures (growth rate, μ_2, decreases
346 from 0.69 (vector) to 0.47 h^{-1}) (**Figure 2C**). Importantly, the spotting control on solid LB media lacking
347 IPTG shows that the size of the inoculum is not affected by potential leaky expression in the overnight
348 culture (**Figure 2B**). Deletion of the RRM renders RelA significantly more toxic (growth rate decreases
349 to 0.29 h^{-1}), in good agreement with the accumulation of (p)ppGpp upon expression of the construct
350 (Turnbull et al., 2019). The effect is countered by TGS H432E, ZFD R629E and even more so by the
351 C612A C613A substitutions (**Figure 2BC**). $RelA^{\Delta RRM}$ expression is equally toxic in the Δ*relA*
352 background and the effect is similarly countered by H432E, R629E and C612A C613A substitutions
353 (**Supplementary Figure S1**), demonstrating that the growth inhibition is independent of the
354 functionality of the endogenous RelA stringent factor. Finally, we directly confirmed the lack of
355 activation by deacylated tRNA in the case of H432E *E. coli* RelA using biochemical assays
356 (**Figure 2D**).

357 Taken together, our results suggest that $RelA^{\Delta RRM}$ toxicity in *E. coli* is dependent on the functionality
358 of the interaction with starved ribosomes. To test the generality of this hypothesis, we next
359 characterised *B. subtilis* Rel lacking the RRM domain.

360 3.2 Toxicity of *B. subtilis* ΔRRM Rel expressed in the $ppGpp^0$ background is mediated by 361 (p)ppGpp synthesis and is countered by mutations compromising the interaction with 362 starved ribosomes

363 We expressed ΔRRM Rel under the control of an IPTG-inducible $P_{hy\text{-}spank}$ promotor (Britton et al.,
364 2002) in $ppGpp^0$ (Δ*rel* Δ*relP* Δ*relQ*) (Nanamiya et al., 2008) or Δ*rel B. subtilis* strains (**Figure 3A**). In
365 the $ppGpp^0$ background, inhibition of *B. subtilis* growth on LB plates is a marker of toxic (p)ppGpp
366 overproduction. In the Δ*rel* background, (p)ppGpp is overproduced by a SAS in the absence of Rel's
367 hydrolytic activity, causing a growth defect in *B. subtilis* (Nanamiya et al., 2008) and *S. aureus* (Geiger
368 et al., 2014). Therefore, this experiment tests the complementation of hydrolase function of Rel that
369 manifests in improved growth.

370 Unlike the full-length Rel, the $Rel^{\Delta RRM}$ truncation is toxic in the $ppGpp^0$ and Δ*rel* backgrounds, both
371 when the growth is followed on plates (**Figure 3A**) and in liquid culture (**Figure 3BC**). To probe the
372 role of the interactions with starved ribosomes in $Rel^{\Delta RRM}$ toxicity, we used a set of substitutions in
373 *B. subtilis* Rel corresponding to those used to study *E. coli* RelA (**Figures 1** and **2**). The toxicity of the
374 $Rel^{\Delta RRM}$ mutant is efficiently countered by the H420E substitution in the TGS as well as the R619E
375 and C602A C603A substitutions in the ZFD (**Figure 3D** and **Supplementary Figure S2D-F, H**). This
376 strongly suggests that the intact interaction with tRNA and starved ribosomes is essential for the
377 toxicity of $Rel^{\Delta RRM}$. For comparison, we tested, full-length Rel, $Rel^{\Delta RRM\Delta ZDF}$ C-terminal truncation, as
378 well as the NTD domain region alone. The $Rel^{\Delta RRM\Delta ZDF}$ mutant is only slightly toxic in the $ppGpp^0$
379 background and its expression promotes growth in the Δ*rel* background (**Figure 3A**). NTD-alone
380 construct displays no toxicity in the $ppGpp^0$ background and does not promote the growth in the Δ*rel*
381 background, suggesting weak – or absent – synthetase activity.

382 To separate the effects of (p)ppGpp production from the effects of (p)ppGpp degradation, we tested
383 synthesis-deficient SYNTH D264G mutants (Nanamiya et al., 2008) of C-terminally truncated Rel
384 variants (**Figure 3A**). The toxicity of the ΔRRM variant is abolished by the D264G mutation
385 demonstrating that it is, indeed, mediated by (p)ppGpp production and not, for example, through
386 inhibition of protein synthesis via competitive binding to ribosomal A-site (the latter non-enzymatic
387 mechanism of toxicity was shown for *E. coli* $RelA^{CTD}$ (Turnbull et al., 2019)). Both ΔRRM D264G

388 and ΔZFDΔRRM D264G variants promote growth in the Δ*rel* strain suggesting that neither deletion
389 of ΔRRM alone – or both ΔZFD and ΔRRM – abrogates the hydrolysis activity of *B. subtilis* Rel
390 (**Figure 3A**, bottom panel). At the same time expression of the synthesis-inactive D264G Rel^{NTD} has
391 no effect, suggesting that the NTD does not efficiently hydrolyse (p)ppGpp. To test if further
392 truncations of the NTD-only Rel (Rel^{1-373}) would induce hydrolytic activity, we tested several
393 additional constructs of *B. subtilis* Rel – Rel^{1-336}, Rel^{1-196} and Rel^{155} – but neither of them could rescue
394 the growth effect of Δ*rel B. subtilis* (**Supplementary Figure S3**). Finally, the synthesis deficiency of
395 D264G Rel and the lack of H420E Rel activation by deacylated tRNA was confirmed using
396 biochemical assays (**Supplementary Figure S4**).

397 Taken together, our results demonstrate that i) $Rel^{\Delta RRM}$ is toxic in $ppGpp^0$ *B. subtilis,* ii) this toxicity
398 requires intact (p)ppGpp synthesis activity of the enzyme iii) it is abrogated by mutations disrupting
399 the interaction with tRNA and starved ribosomes and iv) deletion of the RRM domain does not abrogate
400 the hydrolysis activity of *B. subtilis* Rel.

401 **3.3 The synthetase activity of $Rel^{\Delta RRM}$, $Rel^{\Delta RRM\Delta ZFD}$ and Rel^{NTD} but not the Rel^{H420E} TGS**
402 **mutant can suppress amino acid auxotrophy of $ppGpp^0$ *B. subtilis***

403 To test the low-level, non-toxic, synthesis activity of Rel mutants and to validate the effects of point
404 mutations disrupting the interaction of Rel with starved ribosomal complexes, we took advantage of
405 the amino acid auxotrophy phenotype of the $ppGpp^0$ *B. subtilis* (Δ*rel* Δ*relP* Δ*relQ*) (Nanamiya et al.,
406 2008)).

407 When $ppGpp^0$ *B. subtilis* is grown on Spizizen minimum medium (Spizizen, 1958) in the absence of
408 casamino acids, neither of the D264G Rel mutants – either full-length or C-terminal truncations –
409 promote growth, both whether or not expression is induced by 1 mM IPTG (**Figure 3E**, right panels).
410 Full induction of NTD expression with 1 mM IPTG near-completely supressed the auxotrophy
411 phenotype (**Figure 3E**, top right panel), while the leaky expression in the absence of IPTG results in
412 weak, but detectable suppression (**Figure 3E**, bottom right panel). This demonstrates that *B. subtilis*
413 NTD has a weak net-synthesis activity. The $Rel^{\Delta RRM}$ is, as expected, highly toxic when expression is
414 induced by IPTG; conversely, low-level leakage expression efficiently supresses the amino acid
415 auxotrophy phenotype. Removal of both RRM and ZFD domains renders the protein non-toxic. It is
416 not trivial to reconcile this effect with the idea that removal of the RRM renders the protein toxic due
417 to lack of auto-inhibition: one would expect that the additional removal of the ZFD domain would
418 further compromise the CTD-mediated negative control in $Rel^{\Delta RRM}$.

419 We next used the auxotrophy assay to test the effects of the H420E TGS and C602A C603A ZFD
420 substitutions on the activity of Rel expressed from the native genomic locus under the control of the
421 native promotor (**Figure 3F**). As a positive control we used a strain lacking the genomic copy of *rplK*
422 (*relC*) encoding ribosomal protein L11. This ribosomal element is essential for *E. coli* RelA activation
423 by starved ribosomal complexes (Parker et al., 1976;Wendrich et al., 2002;Shyp et al., 2012) as well
424 as for cellular functionality of *C. crescentus* Rel (Boutte and Crosson, 2011). The $ppGpp^0$ strain
425 expressing H420E Rel fails to grow on the minimum media, reinforcing the crucial role of that this
426 residue, while the C602A C603A can sustain the growth, suggesting that this substitution does not
427 completely abrogate the activity.

428 **3.4 RRM deletion and ZFD mutations destabilise *B. subtilis* Rel binding to starved ribosomal**
429 **complexes**

430 Next, we probed the ribosomal association of ΔRRM and full-length Rel expressed in the ppGpp^0
431 background using a centrifugation sucrose gradient followed by Western blotting using antiserum
432 against native, untagged *B. subtilis* Rel (**Figure 4A**). Since deacylated tRNA promotes ribosomal
433 recruitment of *E. coli* RelA (Agirrezabala et al., 2013;Kudrin et al., 2017), we probed the association
434 of wild type and mutant Rel variants with the ribosome both under exponential growth and upon acute
435 isoleucine starvation induced by the isoleucyl tRNA synthetase inhibitor antibiotic mupirocin
436 (pseudomonic acid) (Thomas et al., 2010). In good agreement with the cryo-EM structures detailing
437 multiple contacts between the RRM and the starved complex and therefore suggesting an importance
438 of this element in ribosomal recruitment (Arenz et al., 2016;Brown et al., 2016;Loveland et al., 2016),
439 we do not detect a stable association of ΔRRM Rel with the ribosome upon a mupirocin challenge.
440 This suggests that the interaction with the ribosome is significantly destabilised in Rel$^{\Delta RRM}$ and the
441 protein dissociates during centrifugation. It is noteworthy that, despite an unstable association of
442 Rel$^{\Delta RRM}$ with starved ribosomes, the expression of this protein strongly induces the accumulation of
443 100S ribosomal dimers, which is indicative of (p)ppGpp overproduction (Tagami et al., 2012). Note
444 that the 100S formation is abrogated when the culture is treated with mupirocin (**Figure 4A** and
445 **Supplementary Figure S5B**), most likely due to complete inhibition of translation by the antibiotic
446 hindering expression of the 100S-promoting Hibernation Promoting Factor (HPF) which, in turn, is
447 induced by accumulation of (p)ppGpp (Tagami et al., 2012).

448 Our microbiological experiments demonstrate that both the C602A and C603A double substitution and
449 the R619E point substitution render Rel$^{\Delta RRM}$ non-toxic (**Figure 3D**), which we attribute to further
450 destabilisation of Rel's interaction with starved ribosomal complexes. To directly probe the effects of
451 these mutations, we used centrifugation experiments with full-length Rel carrying the substitutions. As
452 expected, both the C602A C603A double mutant and R619E full-length variants are compromised in
453 recruitment to the ribosome upon a mupirocin challenge (**Figure 4A**).

454 Taken together, these results demonstrate that Rel$^{\Delta RRM}$ is significantly more toxic than the full-length
455 protein and this toxicity is dependent on the interaction with starved ribosomes, which is, in turn,
456 destabilised in this truncation. As a next step, we set out to test the effects of RRM deletion – either
457 alone or in combination with mutations further compromising the interactions with starved ribosomes
458 – on Rel's enzymatic activity in a reconstituted *B. subtilis* biochemical system.

459 **3.5 Purification of RNA-free untagged *B. subtilis* Rel requires size-exclusion chromatography**

460 To purify untagged *B. subtilis* Rel we combined our protocols used for purification of *E. coli* RelA
461 (Turnbull et al., 2019) and *T. thermophilus* Rel (Van Nerom et al., 2019). (**Figure 5**). Importantly,
462 during all of the chromatography steps we followed both absorbance at 260 and 280 nm complemented
463 with SDS PAGE analysis of fractions. This is essential in order to identify and specifically pool the
464 fractions containing Rel free from RNA contamination. After the initial capture using immobilized
465 metal affinity chromatography (IMAC) in high ionic strength conditions (750 mM KCl) using HisTrap
466 HP column charged with Zn^{2+} in order to avoid possible replacement of the Zn^{2+} in the ZFD domain
467 by Ni^{2+} ions (Block et al., 2009), His_{10}-SUMO-Rel was applied on size-exclusion chromatography
468 (SEC) on HiLoad 16/600 Superdex 200 pg column (**Figure 5D**). Both in the case of the full length
469 (**Figure 5B**) and ΔRRM Rel (**Figure 5C**), the RNA-free fractions constitute the minority of the protein
470 that elute considerably later than the bulk of the RNA-contaminated Rel. While the SEC step is
471 essential for generating RNA-free Rel preparations, the majority of the protein prep is lost at this stage.
472 After the SEC step, the buffer was exchanged to storage buffer containing arginine and glutamic acid
473 that improve protein solubility and long-term stability (Golovanov et al., 2004) (**Figure 5D**), His_{10}-
474 SUMO tag was cleaved off and removed by passing the protein via second IMAC (**Figure 5E**). The

475 quality of the final preparations was assessed by SDS-PAGE (**Figure 5F** and
476 **Supplementary Figure S6**) as well as spectrophotometrically: OD_{260}/OD_{280} ratio below 0.8
477 corresponding to less than 5% RNA contamination (Layne, 1957).

478 We have tested the effects of omission of the SEC step on the purification and activity of *B. subtilis*
479 Rel preparations. Without the SEC step, the OD_{260}/OD_{280} ratio was dramatically higher (1.9),
480 suggesting that, counterintuitively, the 'no SEC' Rel preparation predominantly contains not protein
481 but RNA. We have resolved the sample on 15% SDS-PAGE (**Figure 6A**) and denaturating 1.2%
482 agarose (2% formaldehyde) (**Figure 6B**) gels, as well as subjected the samples to negative staining
483 electron microscopy (**Figure 6C**). While the SDS-PAGE gel revealed multiple protein bands with Mw
484 between 40 and 10 kDa, the agarose gel revealed that the RNA contaminant is dominated by three
485 distinct populations of approximately 3000, 1500 and 100 nucleotides in length. Large (approximately
486 20 nm in diameter) particles are clearly visible on the to negative staining EM images. Collectively,
487 this suggests that the RNA contamination is dominated by ribosomal particles, although it is unclear
488 whether these are intact or partially degraded. Taking into account that 1 A_{260} corresponds to 23 pmol
489 70S particles, we estimate that our 'no SEC' preparations contain 45 nM 70S ribosomes per 1 μM Rel,
490 which corresponds to sub-stoichiometric contamination of 5 % of Rel being in complex, and 95% free.
491 We next tested the effects of SEC omission on the enzymatic activity of Rel. The effects are
492 exceedingly mild. The synthetase activity is virtually unaffected; importantly, activation by deacylated
493 tRNA remains strictly mRNA-dependent, with $tRNA^{Val}$ inducing the enzymatic activity of 'no SEC'
494 Rel only in the presence of 70S initiation complexes (70S IC) but not vacant 70S ribosomes
495 (**Figure 6D**). Importantly, since ribosomes or starved complexes are added in our synthetase assays in
496 excess over Rel (500 nM vs 140 nM Rel), in the final reaction mixture purified ribosomes are in
497 approximately 100x excess over the contaminant. Finally, the hydrolase activity of 'no SEC' Rel is
498 approximately two-fold lower (**Figure 6E**), which, however, could reflect variability in preparations.

499 Taken together, these results suggest that in the absence of a dedicated SEC step, Rel preparations are
500 sub-stoichiometrically contaminated with ribosomes. While the effects of this contamination on the
501 enzymatic activities of Rel are minor, it might interfere with other assays (see *Discussion*).

502 3.6 The R619E ZFD substitution compromises activation of *B. subtilis* $Rel^{\Delta RRM}$ by starved
503 ribosomal complexes

504 We tested the ^{3}H-pppGpp synthesis by full-length Rel as well as $Rel^{\Delta RRM}$, either alone or activated by
505 the ribosomes or starved complexes in a reconstituted system (**Figure 4B**). When the protein is tested
506 by itself, the $Rel^{\Delta RRM}$ mutant is less active than the full-length, suggesting that deletion of the RRM
507 domain does not lead to the loss of auto-inhibition. While $Rel^{\Delta RRM}$ remains less active than the full-
508 length when activated by initiation complexes (about two-fold), in the presence of starved ribosomal
509 complexes the two proteins are equally active. This could be explained by tRNA stabilising Rel on the
510 ribosome and overriding the defect caused by the removal of the RRM domain.

511 The R619E mutation compromises activation of the full-length Rel by the initiation complexes (more
512 than four-fold), and the effect is less pronounced in the presence of deacylated $tRNA^{Val}$ (less than two-
513 fold decrease in activity). Just as in the case of the RRM deletion, a possible explanation is that the
514 deacylated tRNA strongly stimulates the binding of Rel to the ribosome and offsets the effect of the
515 mutation R619E. When the R619E substitution is introduced into ΔRRM Rel, the combination of the
516 two mutations destabilising Rel binding to the ribosome results in compromised activation both by the
517 initiation (five-fold) and starved (seven-fold) ribosomal complex. Despite several attempts we failed

518 to generate sufficiently pure and soluble C602A C603A Rel$^{\Delta RRM}$, which precluded direct biochemical
519 characterisation of this mutant.

520 Taken together, our biochemical results demonstrate that while RRM is important in Rel recruitment
521 to the ribosome, this domain is not absolutely essential for the activation of its (p)ppGpp synthesis
522 activity by starved ribosomal complexes, which is consistent with the ribosome-dependent nature of
523 the Rel$^{\Delta RRM}$ toxicity in live cells.

524 **3.7 The RRM deletion moderately decreases the hydrolysis activity of *B. subtilis* Rel**

525 It was recently proposed that the RRM domain has a stimulatory effect on the hydrolysis activity of
526 *C. crescentus* Rel, and the loss of this regulatory mechanism explains the toxicity of the ΔRRM mutant
527 (Ronneau et al., 2019). This hypothesis does not explain the toxicity of the ΔRRM variant of the
528 synthesis-only RSH RelA (**Figure 2** and (Turnbull et al., 2019)) and our microbiological experiments
529 showing that the synthesis-defective ΔRRM D264G variant of *B. subtilis* Rel remains active as a
530 (p)ppGpp hydrolase (**Figure 3A**). Importantly, the variant characterised by Ronneau and colleagues
531 (*C. crescentus* Rel$^{\Delta 668\text{-}719}$) does not completely lack the RRM, and it is possible that the remaining beta-
532 strand alpha-helix turn structural element was interfering with the hydrolysis activity of the construct
533 (Ronneau et al., 2019).

534 Our enzymatic assays following ^{3}H-pppGpp degradation by full-length and Rel$^{\Delta RRM}$ show that the latter
535 is approximately twice less active (**Figure 4C**). While the defect is detectable, it is quite minor. To test
536 if the hydrolysis defect is more pronounced in the living cell, we re-tested the hydrolysis activity of
537 synthesis-deficient SYNTH D264G full-length Rel as well as C-terminally truncated Rel variants in
538 the Δ*rel* background using the growth rate (μ_2) as a proxy (**Figure 4D**). We modulated the expression
539 levels by titrating the inducer, IPTG, from 10 to 1000 μM. In good agreement with the biochemical
540 results demonstrating a minor defect in hydrolysis caused by deletion of the RRM domain,
541 ΔRRM D264G Rel mutant promotes the growth of Δ*rel B. subtilis* only moderately less efficiently than
542 the full-length D264G.

543 **3.8 The hydrolysis activity of *B. subtilis* Rel is not activated by branched-chain amino acids**
544 **binding to the RRM domain**

545 It was also recently reported that binding of branched-chain amino acids (BCAAs) to the ACT/RRM
546 domain induces the hydrolysis activity of *Rhodobacter capsulatus* Rel (Fang and Bauer, 2018). The
547 N651A substitution abrogates amino acid binding to *R. capsulatus* Rel^{CTD} and leads to (p)ppGpp
548 accumulation in the cell, presumably due to lower hydrolysis activity of the mutant enzyme. It is,
549 therefore, conceivable that *B. subtilis* Rel$^{\Delta RRM}$ is less hydrolytically active in the cell than the full-
550 length protein due to the loss of BCAA-mediated activation. While the *B. subtilis* Rel^{CTD} fragment was
551 shown to preferentially bind leucine with a K_D of 225 μM, no enzymatic assays were performed with
552 this protein (Fang and Bauer, 2018). Notably, while the CTD region of *E. coli* RelA binds valine with
553 high affinity (K_D of 2.85 μM) (Fang and Bauer, 2018), this interaction could not be regulating the
554 hydrolysis activity of this synthesis-only RSH. It is, therefore, unclear whether *B. subtilis* Rel is,
555 indeed, regulated by branched-chain amino acids similarly to *R. capsulatus* enzyme. Therefore, we
556 tested the effect of 1 mM leucine on ^{3}H-pppGpp degradation by *B. subtilis* Rel. We detect no
557 stimulatory effect (**Figure 7A**). Furthermore, when we introduced the N685A substitution (equivalent
558 to N651A in *R. capsulatus*) in the chromosomal *rel* gene, we detected no growth defect in comparison
559 to wild-type 168 *B. subtilis*, either on solid or liquid LB media (**Figure 7B-D**). Taken together, these

560 results suggest that amino acid binding to RRM should not automatically be equated with regulation
561 of the hydrolysis activity.

562

563 **4 Discussion**

564 Taken together, our results demonstrate that i) deletion of the RRM domain renders *B. subtilis* Rel and
565 *E. coli* RelA toxic due to (p)ppGpp overproduction in a ribosome and tRNA-dependent manner, ii)
566 RRM deletion does not abrogate the (p)ppGpp hydrolysis activity of *B. subtilis* Rel, iii) RRM deletion
567 destabilises the interaction of *B. subtilis* Rel with starved ribosomal complexes, and iv) this
568 destabilisation renders the mutant enzyme more sensitive than the full length Rel to deactivation by
569 additional substitutions further compromising its association with starved ribosomes. Our biochemical
570 results do not explain why exactly ΔRRM Rel/RelA is toxic: *B. subtilis* $Rel^{\Delta RRM}$ behaves as a weaker
571 binder of starved ribosomal complexes (**Figure 4A**) and is less enzymatically active in (p)ppGpp
572 synthesis assays (**Figure 4BC**) as compared to the full-length Rel. A dedicated follow-up study is
573 necessary to clarify this question. *E. coli* $RelA^{\Delta RRM}$ displays a similar – although more pronounced –
574 defect in activation by starved ribosomal complexes (Takada et al., 2020).

575 Our report expands the mutation toolbox for dissecting the molecular mechanisms of long RSH
576 enzymes. We confirm that, as was shown for H432E *E. coli* RelA mutant (Winther et al., 2018), the
577 corresponding H420E mutation in *B. subtilis* Rel is a useful tool for specifically abrogating activation
578 of Rel by starved ribosomal complexes. Additionally, we demonstrate the utility of two novel mutations
579 in the ZFD domain: R619E (R629E in *E. coli* RelA) as well as a double C602A C603A substitution
580 (C612A C613A in *E. coli* RelA). While these mutations do not completely abrogate the activation,
581 acting in epistasis they can be employed to reveal weaker phenotypes or effects, as was shown in the
582 current work when the mutations were combined with RRM/ACT deletion.

583 Finally, we would like to draw the attention of the research community working on long RSH enzymes
584 to technical aspects of protein purification. It is common to purify Rel/RelA for biochemical
585 experiments using a single-step purification (for example (Gratani et al., 2018;Wood et al., 2019)).
586 However, both RelA (Turnbull et al., 2019) and Rel have a strong tendency for RNA contamination
587 and multiple additional steps are necessary to remove this contaminant. Therefore, reporting the
588 260/280 absorbance ratio of the final preparations is essential. RNA-free protein preparations typically
589 have a 260/280 absorbance ratio of 0.57, but this parameter can vary depending on the amino acid
590 composition, specifically the abundance of tryptophan and phenylalanine (Layne, 1957). Without extra
591 steps to remove RNA contamination, single-step preparations are likely to be heavily contaminated
592 with ribosomal particles (**Figure 6**), which is likely to interfere with the estimation of the
593 oligomerisation state of Rel, since the RNA-bound protein elutes much earlier than the RNA-free
594 fraction (**Figure 5BC**). This contamination may explain the surprising observation that the addition of
595 Ni-NTA purified *S. aureus* Rel inhibits the 50S assembly factor DEAD-box RNA helicase CshA
596 (Wood et al., 2019). The unlabelled contaminating ribosomal particles could potentially be recognised
597 by CshA, thus acting as a competitor in the helicase assay that uses a synthetic Cy3-labelled RNA
598 duplex as a substrate. It is also plausible that formation of stable complexes of Rel with ribosomes in
599 live *E. coli* could generate false-positive signals in bacterial two-hybrid assays, accounting for the
600 observed protein-protein interaction between *S. aureus* Rel and the ribosome assembly factors Era and
601 CshA (Wood et al., 2019).

602 **5 References**

603 Agirrezabala, X., Fernandez, I.S., Kelley, A.C., Carton, D.G., Ramakrishnan, V., and Valle, M. (2013).
604 The ribosome triggers the stringent response by RelA via a highly distorted tRNA. *EMBO Rep*
605 14**,** 811-816.

606 Akanuma, G., Kazo, Y., Tagami, K., Hiraoka, H., Yano, K., Suzuki, S., Hanai, R., Nanamiya, H., Kato-
607 Yamada, Y., and Kawamura, F. (2016). Ribosome dimerization is essential for the efficient
608 regrowth of *Bacillus subtilis*. *Microbiology* 162**,** 448-458.

609 Antoun, A., Pavlov, M.Y., Tenson, T., and Ehrenberg, M.M. (2004). Ribosome formation from
610 subunits studied by stopped-flow and Rayleigh light scattering. *Biol Proced Online* 6**,** 35-54.

611 Arenz, S., Abdelshahid, M., Sohmen, D., Payoe, R., Starosta, A.L., Berninghausen, O., Hauryliuk, V.,
612 Beckmann, R., and Wilson, D.N. (2016). The stringent factor RelA adopts an open
613 conformation on the ribosome to stimulate ppGpp synthesis. *Nucleic Acids Res* 44**,** 6471-6481.

614 Atkinson, G.C., Tenson, T., and Hauryliuk, V. (2011). The RelA/SpoT homolog (RSH) superfamily:
615 distribution and functional evolution of ppGpp synthetases and hydrolases across the tree of
616 life. *PLoS One* 6**,** e23479.

617 Avarbock, A., Avarbock, D., Teh, J.S., Buckstein, M., Wang, Z.M., and Rubin, H. (2005). Functional
618 regulation of the opposing (p)ppGpp synthetase/hydrolase activities of RelMtb from
619 *Mycobacterium tuberculosis*. *Biochemistry* 44**,** 9913-9923.

620 Avarbock, D., Avarbock, A., and Rubin, H. (2000). Differential regulation of opposing RelMtb
621 activities by the aminoacylation state of a tRNA.ribosome.mRNA.RelMtb complex.
622 *Biochemistry* 39**,** 11640-11648.

623 Beljantseva, J., Kudrin, P., Andresen, L., Shingler, V., Atkinson, G.C., Tenson, T., and Hauryliuk, V.
624 (2017). Negative allosteric regulation of *Enterococcus faecalis* small alarmone synthetase RelQ
625 by single-stranded RNA. *Proc Natl Acad Sci U S A* 114**,** 3726-3731.

626 Block, H., Maertens, B., Spriestersbach, A., Brinker, N., Kubicek, J., Fabis, R., Labahn, J., and Schafer,
627 F. (2009). Immobilized-metal affinity chromatography (IMAC): a review. *Methods Enzymol*
628 463**,** 439-473.

629 Boutte, C.C., and Crosson, S. (2011). The complex logic of stringent response regulation in
630 *Caulobacter crescentus*: starvation signalling in an oligotrophic environment. *Mol Microbiol*
631 80**,** 695-714.

632 Britton, R.A., Eichenberger, P., Gonzalez-Pastor, J.E., Fawcett, P., Monson, R., Losick, R., and
633 Grossman, A.D. (2002). Genome-wide analysis of the stationary-phase sigma factor (sigma-H)
634 regulon of *Bacillus subtilis*. *J Bacteriol* 184**,** 4881-4890.

635 Brodiazhenko, T., Johansson, M.J.O., Takada, H., Nissan, T., Hauryliuk, V., and Murina, V. (2018).
636 Elimination of Ribosome Inactivating Factors Improves the Efficiency of *Bacillus subtilis* and
637 *Saccharomyces cerevisiae* Cell-Free Translation Systems. *Front Microbiol* 9**,** 3041.

638 Brown, A., Fernandez, I.S., Gordiyenko, Y., and Ramakrishnan, V. (2016). Ribosome-dependent
639 activation of stringent control. *Nature* 534**,** 277-280.

640 Dalebroux, Z.D., Svensson, S.L., Gaynor, E.C., and Swanson, M.S. (2010). ppGpp conjures bacterial
641 virulence. *Microbiol Mol Biol Rev* 74**,** 171-199.

642 Dalebroux, Z.D., and Swanson, M.S. (2012). ppGpp: magic beyond RNA polymerase. *Nat Rev*
643 *Microbiol* 10**,** 203-212.

644 Fang, M., and Bauer, C.E. (2018). Regulation of stringent factor by branched-chain amino acids. *Proc*
645 *Natl Acad Sci U S A* 115**,** 6446-6451.

646 Geiger, T., Kastle, B., Gratani, F.L., Goerke, C., and Wolz, C. (2014). Two small (p)ppGpp synthases
647 in *Staphylococcus aureus* mediate tolerance against cell envelope stress conditions. *J Bacteriol*
648 196**,** 894-902.

649 Golovanov, A.P., Hautbergue, G.M., Wilson, S.A., and Lian, L.Y. (2004). A simple method for
650 improving protein solubility and long-term stability. *J Am Chem Soc* 126**,** 8933-8939.

651 Gratani, F.L., Horvatek, P., Geiger, T., Borisova, M., Mayer, C., Grin, I., Wagner, S., Steinchen, W.,
652 Bange, G., Velic, A., Macek, B., and Wolz, C. (2018). Regulation of the opposing (p)ppGpp
653 synthetase and hydrolase activities in a bifunctional RelA/SpoT homologue from
654 *Staphylococcus aureus*. *PLoS Genet* 14**,** e1007514.

655 Gropp, M., Strausz, Y., Gross, M., and Glaser, G. (2001). Regulation of *Escherichia coli* RelA requires
656 oligomerization of the C-terminal domain. *J Bacteriol* 183**,** 570-579.

657 Haseltine, W.A., and Block, R. (1973). Synthesis of guanosine tetra- and pentaphosphate requires the
658 presence of a codon-specific, uncharged transfer ribonucleic acid in the acceptor site of
659 ribosomes. *Proc Natl Acad Sci U S A* 70**,** 1564-1568.

660 Hauryliuk, V., Atkinson, G.C., Murakami, K.S., Tenson, T., and Gerdes, K. (2015). Recent functional
661 insights into the role of (p)ppGpp in bacterial physiology. *Nat Rev Microbiol* 13**,** 298-309.

662 Inabe, T. (2005). Mellitate anions: unique anionic component with supramolecular self-organizing
663 properties. *Journal of Materials Chemistry* 15**,** 1317-1328.

664 Jiang, M., Sullivan, S.M., Wout, P.K., and Maddock, J.R. (2007). G-protein control of the ribosome-
665 associated stress response protein SpoT. *J Bacteriol* 189**,** 6140-6147.

666 Jimmy, S., Saha, C.K., Stavropoulos, C., Garcia-Pino, A., Hauryliuk, V., and Atkinson, G.C. (2019).
667 Discovery of small alarmone synthetases and their inhibitors as toxin-antitoxin loci. *bioXriv***,**
668 DOI: 10.1101/575399.

669 Katoh, K., and Standley, D.M. (2013). MAFFT multiple sequence alignment software version 7:
670 improvements in performance and usability. *Mol Biol Evol* 30**,** 772-780.

671 Kudrin, P., Dzhygyr, I., Ishiguro, K., Beljantseva, J., Maksimova, E., Oliveira, S.R.A., Varik, V.,
672 Payoe, R., Konevega, A.L., Tenson, T., Suzuki, T., and Hauryliuk, V. (2018). The ribosomal
673 A-site finger is crucial for binding and activation of the stringent factor RelA. *Nucleic Acids*
674 *Res* 46**,** 1973-1983.

675 Kudrin, P., Varik, V., Oliveira, S.R., Beljantseva, J., Del Peso Santos, T., Dzhygyr, I., Rejman, D.,
676 Cava, F., Tenson, T., and Hauryliuk, V. (2017). Subinhibitory Concentrations of Bacteriostatic
677 Antibiotics Induce *relA*-Dependent and *relA*-Independent Tolerance to beta-Lactams.
678 *Antimicrob Agents Chemother* 61.

679 Kushwaha, G.S., Oyeyemi, B.F., and Bhavesh, N.S. (2019). Stringent response protein as a potential
680 target to intervene persistent bacterial infection. *Biochimie* 165**,** 67-75.

681 Layne, E. (1957). Spectrophotometric and Turbidimetric Methods for Measuring Proteins. *Methods in*
682 *Enzymology* 3**,** 447-454.

683 Liu, K., Bittner, A.N., and Wang, J.D. (2015). Diversity in (p)ppGpp metabolism and effectors. *Curr*
684 *Opin Microbiol* 24**,** 72-79.

685 Loveland, A.B., Bah, E., Madireddy, R., Zhang, Y., Brilot, A.F., Grigorieff, N., and Korostelev, A.A.
686 (2016). Ribosome*RelA structures reveal the mechanism of stringent response activation. *eLife*
687 5.

688 Mechold, U., Murphy, H., Brown, L., and Cashel, M. (2002). Intramolecular regulation of the opposing
689 (p)ppGpp catalytic activities of Rel(Seq), the Rel/Spo enzyme from *Streptococcus equisimilis*.
690 *J Bacteriol* 184**,** 2878-2888.

691 Mittenhuber, G. (2001). Comparative genomics and evolution of genes encoding bacterial (p)ppGpp
692 synthetases/hydrolases (the Rel, RelA and SpoT proteins). *J Mol Microbiol Biotechnol* 3**,** 585-
693 600.

694 Molin, S., Stougaard, P., Uhlin, B.E., Gustafsson, P., and Nordstrom, K. (1979). Clustering of genes
695 involved in replication, copy number control, incompatibility, and stable maintenance of the
696 resistance plasmid R1drd-19. *J Bacteriol* 138**,** 70-79.

697 Murina, V., Kasari, M., Hauryliuk, V., and Atkinson, G.C. (2018a). Antibiotic resistance ABCF
698 proteins reset the peptidyl transferase centre of the ribosome to counter translational arrest.
699 *Nucleic Acids Res* 46**,** 3753-3763.

700 Murina, V., Kasari, M., Takada, H., Hinnu, M., Saha, C.K., Grimshaw, J.W., Seki, T., Reith, M.,
701 Putrins, M., Tenson, T., Strahl, H., Hauryliuk, V., and Atkinson, G.C. (2018b). ABCF ATPases
702 Involved in Protein Synthesis, Ribosome Assembly and Antibiotic Resistance: Structural and
703 Functional Diversification across the Tree of Life. *J Mol Biol*. 431(18)**,** 3568-3590

704 Nanamiya, H., Kasai, K., Nozawa, A., Yun, C.S., Narisawa, T., Murakami, K., Natori, Y., Kawamura,
705 F., and Tozawa, Y. (2008). Identification and functional analysis of novel (p)ppGpp synthetase
706 genes in *Bacillus subtilis*. *Mol Microbiol* 67**,** 291-304.

707 Parker, J., Watson, R.J., and Friesen, J.D. (1976). A relaxed mutant with an altered ribosomal protein
708 L11. *Mol Gen Genet* 144**,** 111-114.

709 Ronneau, S., Caballero-Montes, J., Coppine, J., Mayard, A., Garcia-Pino, A., and Hallez, R. (2019).
710 Regulation of (p)ppGpp hydrolysis by a conserved archetypal regulatory domain. *Nucleic Acids*
711 *Res* 47**,** 843-854.

712 Schreiber, G., Metzger, S., Aizenman, E., Roza, S., Cashel, M., and Glaser, G. (1991). Overexpression
713 of the relA gene in E*scherichia coli*. *J Biol Chem* 266**,** 3760-3767.

714 Shyp, V., Tankov, S., Ermakov, A., Kudrin, P., English, B.P., Ehrenberg, M., Tenson, T., Elf, J., and
715 Hauryliuk, V. (2012). Positive allosteric feedback regulation of the stringent response enzyme
716 RelA by its product. *EMBO Rep* 13**,** 835-839.

717 Spizizen, J. (1958). Transformation of Biochemically Deficient Strains of *Bacillus subtilis* by
718 Deoxyribonucleate. *Proc Natl Acad Sci U S A* 44**,** 1072-1078.

719 Steinchen, W., and Bange, G. (2016). The magic dance of the alarmones (p)ppGpp. *Mol Microbiol*
720 101**,** 531-544.

721 Tagami, K., Nanamiya, H., Kazo, Y., Maehashi, M., Suzuki, S., Namba, E., Hoshiya, M., Hanai, R.,
722 Tozawa, Y., Morimoto, T., Ogasawara, N., Kageyama, Y., Ara, K., Ozaki, K., Yoshida, M.,
723 Kuroiwa, H., Kuroiwa, T., Ohashi, Y., and Kawamura, F. (2012). Expression of a small
724 (p)ppGpp synthetase, YwaC, in the (p)ppGpp(0) mutant of *Bacillus subtilis* triggers YvyD-
725 dependent dimerization of ribosome. *Microbiologyopen* 1**,** 115-134.

726 Takada, H., Roghanian, M., Caballero-Montes, J., Van Nerom, K., Jimmy, S., Kudrin, P., Trebibi, F.,
727 Murayama, R., Akanuma, G., Garcia-Pino, A., and Hauryliuk, V. (2020). Ribosome association

primes the stringent factor Rel for recruitment of deacylated tRNA to ribosomal A-site. *bioRxiv*. DOI: 10.1101/2020.01.17.910273.

Tamman, H., Van Nerom, K., Takada, H., Vandenberk, S., Polikanov, Y., Hofkens, J., Talavera, A., Hauryliuk, V., Hendrix, J., and Garcia-Pino, A. (2019). Nucleotide-mediated allosteric regulation of bifunctional Rel enzymes. *bioRxiv* DOI: 10.1101/670703.

Thomas, C.M., Hothersall, J., Willis, C.L., and Simpson, T.J. (2010). Resistance to and synthesis of the antibiotic mupirocin. *Nat Rev Microbiol* 8**,** 281-289.

Turnbull, K.J., Dzhygyr, I., Lindemose, S., Hauryliuk, V., and Roghanian, M. (2019). Intramolecular Interactions Dominate the Autoregulation of *Escherichia coli* Stringent Factor RelA. *Front Microbiol* 10**,** 1966.

Van Nerom, K., Tamman, H., Takada, H., Hauryliuk, V., and Garcia-Pino, A. (2019). The Rel stringent factor from *Thermus thermophilus*: crystallization and X-ray analysis. *Acta Crystallogr F Struct Biol Commun* 75**,** 561-569.

Waterhouse, A.M., Procter, J.B., Martin, D.M., Clamp, M., and Barton, G.J. (2009). Jalview Version 2--a multiple sequence alignment editor and analysis workbench. *Bioinformatics* 25**,** 1189-1191.

Wendrich, T.M., Blaha, G., Wilson, D.N., Marahiel, M.A., and Nierhaus, K.H. (2002). Dissection of the mechanism for the stringent factor RelA. *Mol Cell* 10**,** 779-788.

Wilkinson, R.C., Batten, L.E., Wells, N.J., Oyston, P.C., and Roach, P.L. (2015). Biochemical studies on *Francisella tularensis* RelA in (p)ppGpp biosynthesis. *Biosci Rep* 35.

Winther, K.S., Roghanian, M., and Gerdes, K. (2018). Activation of the Stringent Response by Loading of RelA-tRNA Complexes at the Ribosomal A-Site. *Mol Cell* 70**,** 95-105 e104.

Wood, A., Irving, S.E., Bennison, D.J., and Corrigan, R.M. (2019). The (p)ppGpp-binding GTPase Era promotes rRNA processing and cold adaptation in *Staphylococcus aureus*. *PLoS Genet* 15**,** e1008346.

Xiao, H., Kalman, M., Ikehara, K., Zemel, S., Glaser, G., and Cashel, M. (1991). Residual guanosine 3',5'-bispyrophosphate synthetic activity of *relA* null mutants can be eliminated by *spoT* null mutations. *J Biol Chem* 266**,** 5980-5990.

Yang, N., Xie, S., Tang, N.Y., Choi, M.Y., Wang, Y., and Watt, R.M. (2019). The Ps and Qs of alarmone synthesis in *Staphylococcus aureus*. *PLOS One* 14**,** e0213630.

6 Conflict of Interest

The authors declare that the research was conducted in the absence of any commercial or financial relationships that could be construed as a potential conflict of interest.

7 Author Contributions

HT conceived the study, HT, MR and VH designed experiments, HT performed experiments with *B. subtilis* Rel, ID and MR performed experiments with *E. coli* RelA, VM performed electron microscopy, RM and GA contributed tools and reagents, GCA and AG-P performed structure and sequence analyses, HT and VH drafted and revised the manuscript with contributions from MR, AG-P and GCA. All authors have read and approved the final version of this manuscript.

8 Funding

768 This work was supported by the European Regional Development Fund through the Centre of
769 Excellence for Molecular Cell Technology (VH), the Molecular Infection Medicine Sweden (MIMS)
770 (VH), Swedish Research council (grant 2017-03783 to VH and grant 2015-04746 to GCA), Ragnar
771 Söderberg foundation (VH), Umeå Centre for Microbial Research (UCMR) (postdoctoral grant 2017
772 to HT), MIMS Excellence by Choice Postdoctoral Fellowship Programme (MR), the Fonds National
773 de Recherche Scientifique (grants FRFS-WELBIO CR-2017S-03, FNRS CDR J.0068.19 and FNRS-
774 PDR T.0066.18 to AG-P) and the Fonds Jean Brachet and the Fondation Van Buuren (AG-P).

775 **9 Acknowledgments**

776 We would like to thank the Protein Expertise Platform (PEP) at Umeå University and Mikael Lindberg
777 for constructing pET24d::*His*$_{10}$-*SUMO*-based expression constructs and purifying His$_6$-Ulp1, and
778 Julien Caballero-Montes for comments on the manuscript. The electron microscopy data was collected
779 at the Umeå Core Facility for Electron Microscopy, a node of the Cryo-EM Swedish National Facility,
780 funded by the Knut and Alice Wallenberg, Family Erling Persson and Kempe Foundations, SciLifeLab,
781 Stockholm University and Umeå University.

782

783 **10 Figures**

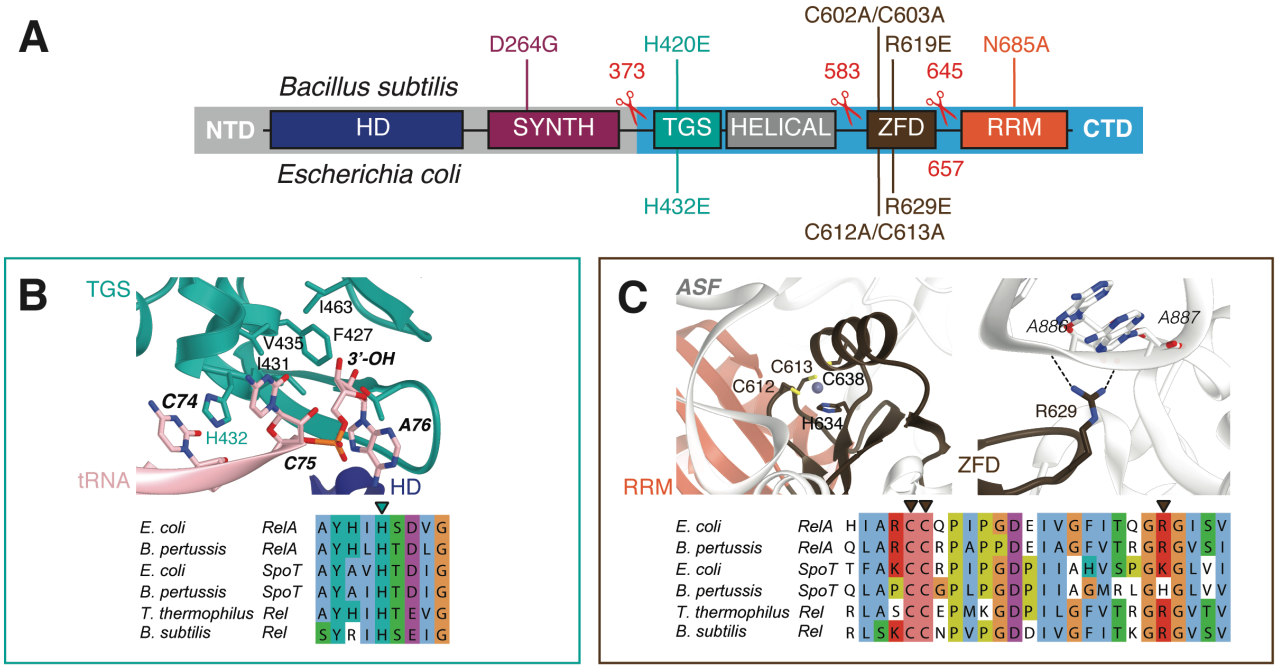

784

785 **Figure 1. Domain structure of 'long' ribosome-associated RSHs Rel and RelA.** (**A**) The NTD
786 region contains (p)ppGpp hydrolysis (HD) and (p)ppGpp synthesis (SYNTH) NTD domains. TGS
787 (ThrRS, GTPase and SpoT), Helical, ZFD (Zinc Finger Domain) and RRM (RNA Recognition Motif)
788 domains comprise the regulatory CTD region. Mutations and truncations of *B. subilis* Rel and *E. coli*
789 RelA used in this study are indicated above and below the domain schematics, respectively. (**B**)
790 Conservation and structural environment of mutations in the TGS domain used in the current study.
791 (**C**) Conservation and structural environment of mutations in the RRM domain used in the current
792 study. The 3D structures are as per from Loveland and colleagues (Loveland et al., 2016), RDB
793 accession number 5KPX.

794

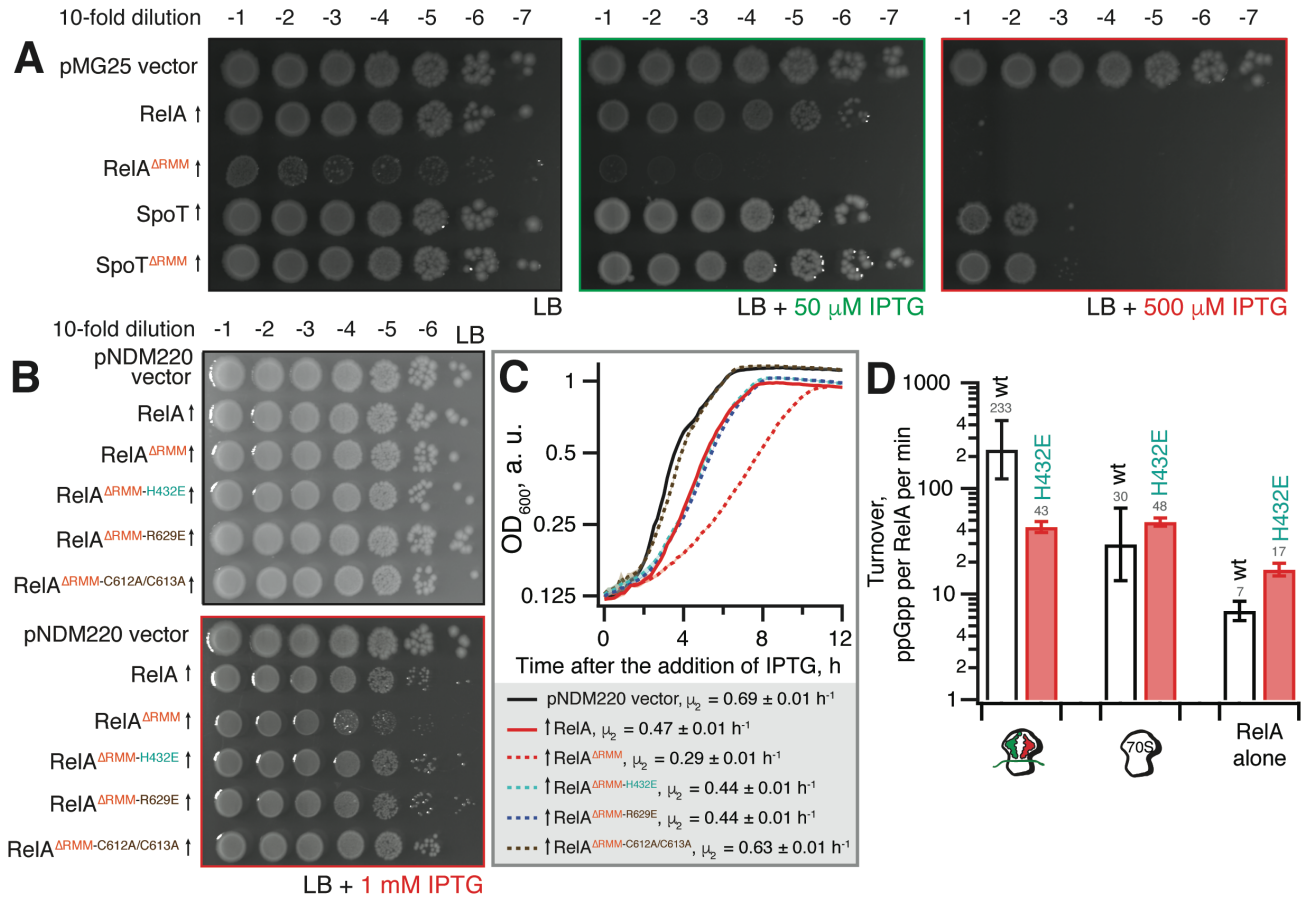

Figure 2. The toxicity of ΔRRM *E. coli* RelA is mitigated by mutations compromising interactions with tRNA and the ribosome. (**A**) Wild-type *E. coli* BW25113 cells were transformed with either the empty high-copy IPTG-inducible pMG25 plasmid vector or pMG25-based constructs expressing wild-type and ΔRRM versions of *E. coli* RelA and SpoT. Up-pointing arrows indicate induction of expression. Ten-fold serial dilutions of overnight LB cultures were made and spotted onto LB agar supplemented with 100 μg/mL ampicillin and either 0, 50 or 500 μM IPTG. The plates were incubated at 37 °C and scored after 18 hours. (**B**) *E. coli* BW25113 cells were transformed either with the empty low-copy IPTG-inducible pNDM220 vector or pNDM220-based constructs expressing wild-type and mutant versions of *E. coli* RelA as indicated on the figure. Ten-fold serial dilutions of overnight LB cultures were made and spotted onto LB agar supplemented with 30 μg/mL ampicillin and 1 mM IPTG. As a plating control the same dilutions of the overnight cultures were spotted on LB agar supplemented with 30 μg/mL ampicillin but no IPTG. The plates were incubated at 37 °C and scored after 18 hours. (**C**) Thousand-fold dilutions of the same overnights were made in LB supplemented with 30 μg/mL ampicillin and 1 mM IPTG, and growth at 37 °C was monitored using the Bioscreen C growth curve analysis system. The growth rates (μ^2) were calculated from three independent measurements and the error bars represent standard errors. (**D**) H432E TGS *E. coli* RelA is not activated by deacylated tRNA on the ribosome. The synthetase activity of 30 nM wild type and H432E *E. coli* RelA was assayed in the presence of 1 mM ATP, 300 μM ^{3}H GDP and 100 μM ppGpp in HEPES:Polymix buffer, pH 7.5, 37 °C, 5 mM Mg^{2+}. As indicated on the figure, the reaction mixture was supplemented either with 2 μM vacant 70S ribosomes or with an *in situ* assembled starved ribosomal complex (2 μM vacant 70S combined with 2 μM mRNA(MV), 2 μM *E. coli* $tRNA_i^{fMet}$ and 2 μM *E. coli* $tRNA^{Val}$). The error bars represent standard deviations of the turnover estimates by linear regression using four data points.

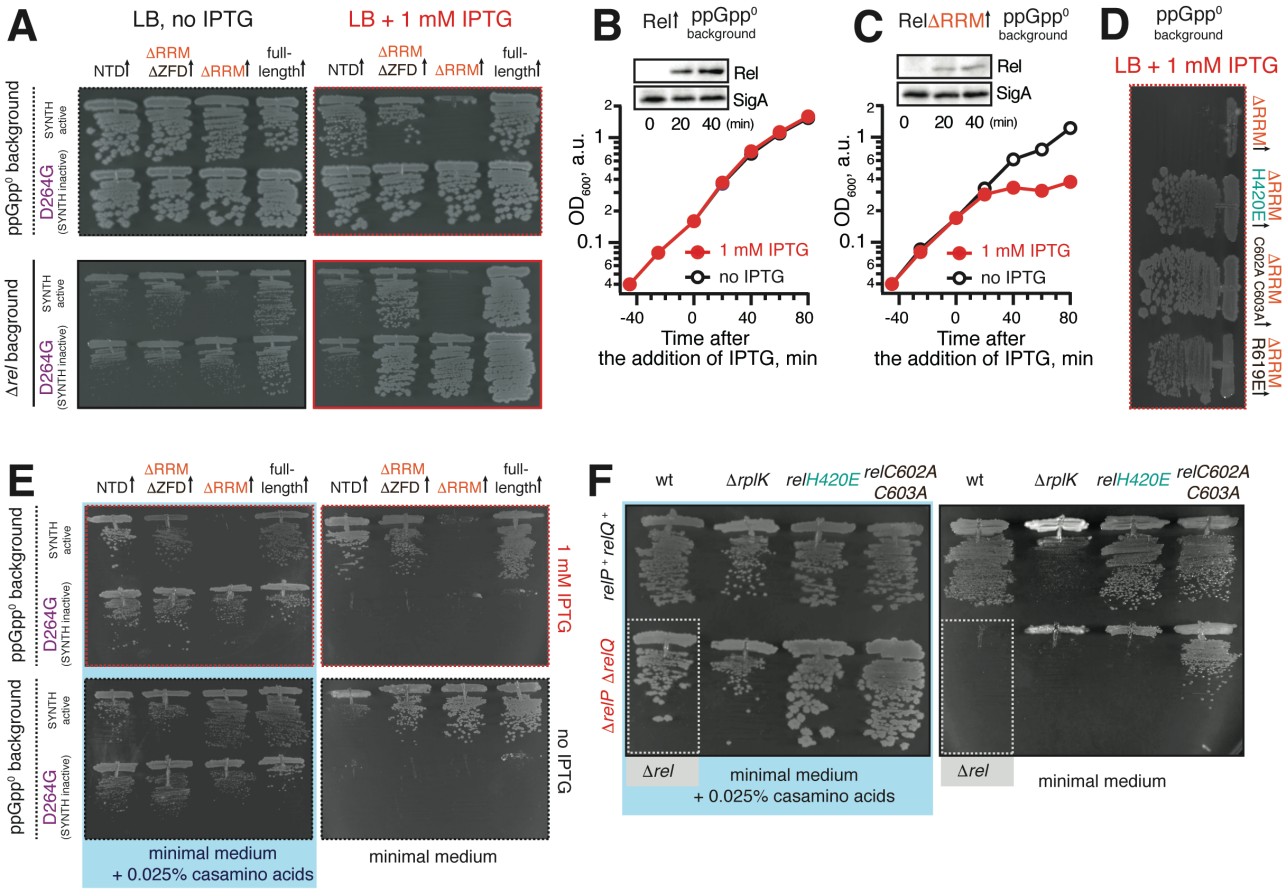

Figure 3. Deletion of the regulatory RRM domain leads to *B. subtilis* Rel toxicity due to ribosome-dependent (p)ppGpp overproduction. (**A**) Full-length (VHB155 and VHB183) as well as C-terminally truncated Rel variants [synthesis-competent ΔRRM (VHB159 and VHB184), ΔRRMΔZFD (VHB160 and VHB185) and Rel^{NTD} (VHB161 and VHB186), and the corresponding synthesis-inactive D264G mutants VHB162-164; VHB187-190] were expressed in either $ppGpp^0$ (upper row; test for toxicity mediated by (p)ppGpp accumulation) or Δ*rel* (lower row; test for HD functionality) *B. subtilis* growing on solid LB medium. Up-pointing arrows (↑) indicate ectopic expression. (**B-C**) Expression of $Rel^{\Delta RRM}$ causes a growth defect in liquid culture. Either wild-type *rel* (VHB183) (**B**) or $rel^{\Delta RRM}$ mutant (VHB184) (**C**) were expressed in $ppGpp^0$ background grown in liquid LB medium at 37 °C. Protein expression was induced by IPTG added to final concentration of 1 mM to exponentially growing bacterial cultures at OD_{600} 0.2. Protein expression was monitored by Western blotting using anti-Rel antibodies (see also **Supplementary Figure S2H**). (**D**) The toxicity of mutant versions of $Rel^{\Delta RRM}$ tested in $ppGpp^0$ *B. subtilis* growing on solid LB medium: wild type $Rel^{\Delta RRM}$ (VHB184), H420E (VHB231) defective in recognition of the tRNA 3' CCA end, and ZFD mutants C602A C603A (VHB233) and R619E (VHB281) defective in 70S binding. LB plates were scored after 18 hour incubation at 37 °C. (**E**) C-terminally truncated Rel variants (either synthesis-competent (VHB155, VHB159-161) or synthesis-inactive D264G mutant versions (VHB156, VHB162-164)) were expressed in $ppGpp^0$ *B. subtilis* growing on either solid minimal medium or solid minimal medium supplemented with 0.025% casamino acids. Plates were scored after 36 hours incubation at 37 °C. Importantly, prior to experiment all strains were pre-cultured on solid minimal medium supplemented with 0.025% casamino acids. This was done in order to avoid the effects caused by the decreased fitness of the inoculum. (**F**) Synthesis activity of Rel mutants probed by amino acid auxotrophy assays. *B. subtilis* strains were constructed using either $relP^+$ $relQ^+$ wild-type 168 (upper row) or Δ*relP* Δ*relP* (lower

843 row) background. The strains either expressed the indicated *rel* mutants (H420E (VHB68) and
844 C602A C603A (VHB148), upper row, and H420E (VHB60), C602A C603A (VHB62), lower row) or
845 contained an additional Δ*rplK* gene disruption (VHB47, $relP^+$ $relQ^+$ and VHB49, Δ*relP* Δ*relP*). The
846 $ppGpp^0$ mutant strain (Δ*relP* Δ*relP* Δ*rel*, VHB63) was used as a control (highlighted with grey box).
847 The strains were grown on either solid Spizizen minimal medium (right panel) or solid minimal
848 medium supplemented with 0.025% casamino acids (left panel).

849

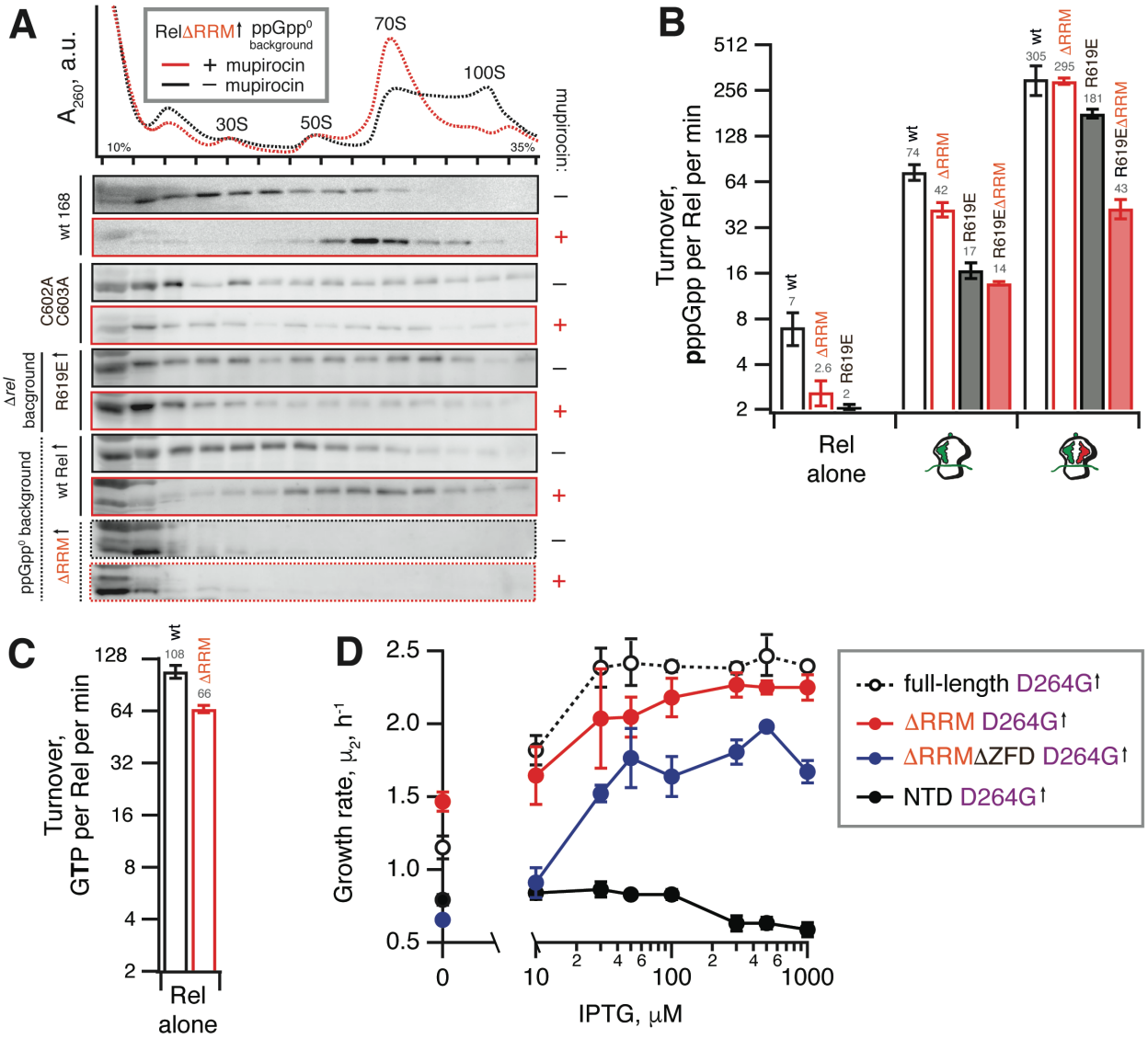

Figure 4. Deletion of the regulatory RRM domain destabilises Rel binding to starved ribosomal complexes and does not abrogate the hydrolysis activity. (**A**) Polysome profile and immunoblot analyses of Rel variants expressed either ectopically (↑) under the control of IPTG-inducible $P_{hy\text{-}spnak}$ promotor [ΔRRM Rel in ppGpp⁰ *B. subtilis* (VHB184), R619E Rel in Δ*rel B. subtilis* (VHB282)] or from the native chromosomal locus [C602A C603A mutant (VHB144)]. Expression of $Rel^{\Delta RRM}$ was induced by 1 mM IPTG for 10 minutes followed by a 10 minute challenge with 700 nM mupirocin. To drive the expression of R619E Rel, the strain as grown in LB supplemented with 1 mM IPTG. In the case of R619E and C602A C603A Rel the culture was treated with mupirocin for 20 minutes. Polysome profiles of all tested Rel variants are presented in **Supplementary Figure S5**, and an uncut version of a representative anti-Rel immunoblot is shown in **Supplementary Figure S2G**. (**B** and **C**) The effect of the RRM deletion on synthetic (**B**) and hydrolytic activity (**C**). The effects of the RRM deletion and the R619E mutation on Rel synthetic activity were assayed either alone or in the presence of either initiation and starved ribosomal complexes. The error bars represent standard deviations of the turnover estimates by linear regression using four data points. (**D**) The effects of titratable expression of synthesis-inactive D264G mutants (full-length VHB156, ΔRRM VHB162, ΔRRMΔZFD VHB163 and Rel^{NTD} VHB164) on Δ*rel B. subtilis* growing on liquid LB medium at 37 °C. The growth rates (μ^2)

867 were calculated from three independent biological replicates and the error bars represent standard
868 deviations.

869

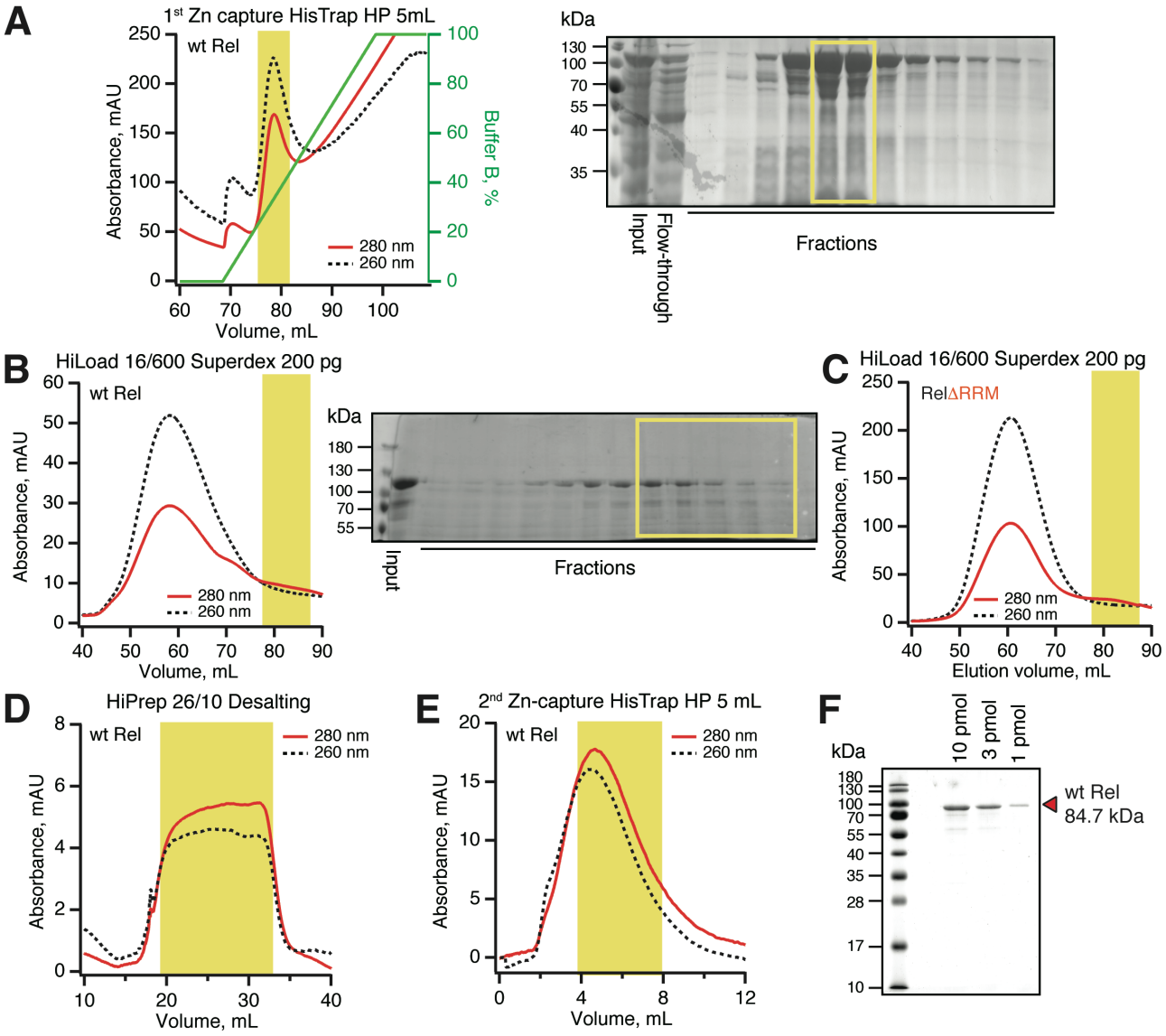

Figure 5. Purification of RNA-free untagged *B. subtilis* Rel. N-terminally His_{10}-SUMO tagged RelA was overexpressed and purified as described in detail in *Materials and Methods*. (**A**) Cells were lysed and subjected to immobilized metal affinity chromatography (IMAC) using a Zn^{2+}-charged HisTrap 5 mL HP column. The fraction corresponding to Rel with the lowest contamination of nucleic acids (highlighted in yellow) was carried forward. Size-exclusion chromatography on HiLoad 16/600 Superdex 200 pg was used to further separate the RNA-free Rel fractions (**B**: full-length wild type Rel; **C**: ΔRRM Rel). Following the buffer exchange on HiPrep 10/26 desalting column (**D**), the boxed-out fractions were pooled and the His_{10}-SUMO tag was cleaved off by the His_6-Ulp1 protease. (**E**) Native untagged Rel was separated from His_6-Ulp1 and the His_{10}-SUMO tag by the second round of IMAC. Highlighted fractions were pooled, concentrated, aliquoted, flash-frozen in liquid nitrogen and stored at –80 °C. (**F**) SDS-PAGE analysis of the purified native untagged *B. subtilis* Rel.

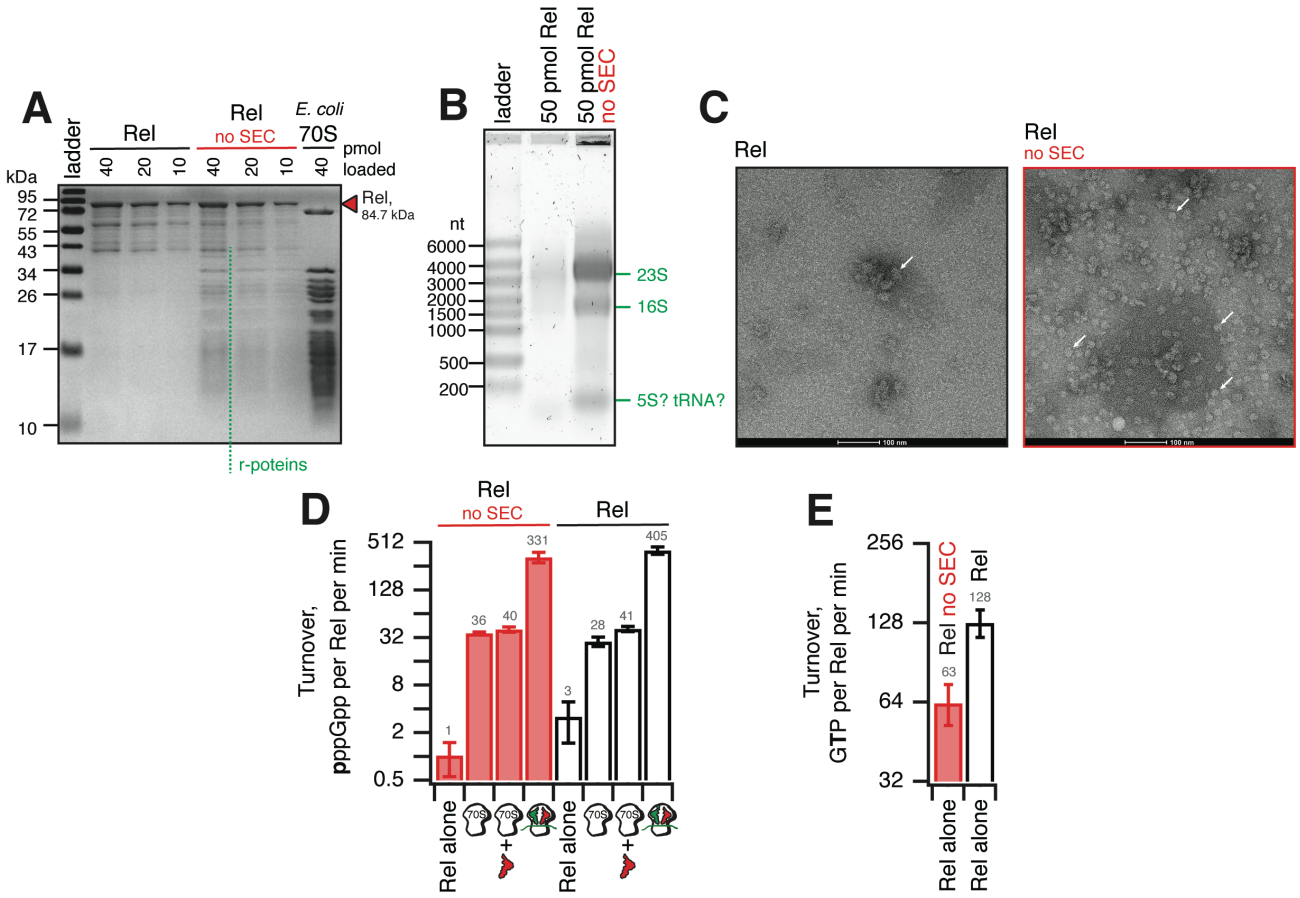

Figure 6. Omission of the size-exclusion chromatography step results in sub-stoichiometric contamination of *B. subtilis* Rel preparations with *E. coli* ribosomal particles. (**A**) SDS-PAGE analysis of wild-type full-length Rel protein purified either as described in **Figure 5** or with the SEC step omitted (no SEC). Desaturating agarose gel (**B**) and negative staining electron microscopy (**C**) analyses of full-length Rel protein purified with and without the SEC step. Individual ribosomal particles are indicated with white arrows on (**C**). Effects of the SEC omission on synthetase (**D**) and hydrolase (**E**) activity of *B. subtilis* Rel. The synthetase activity was assayed with either Rel alone or in the presence of 0.5 μM 70S, 70S supplemented with 2 μM deacylated $tRNA^{Val}$ and no mRNA or starved ribosomal complexes (0.5 μM 70S IC(MVF) supplemented with 2 μM deacylated $tRNA^{Val}$). The error bars represent standard deviations of the turnover estimates by linear regression using four data points.

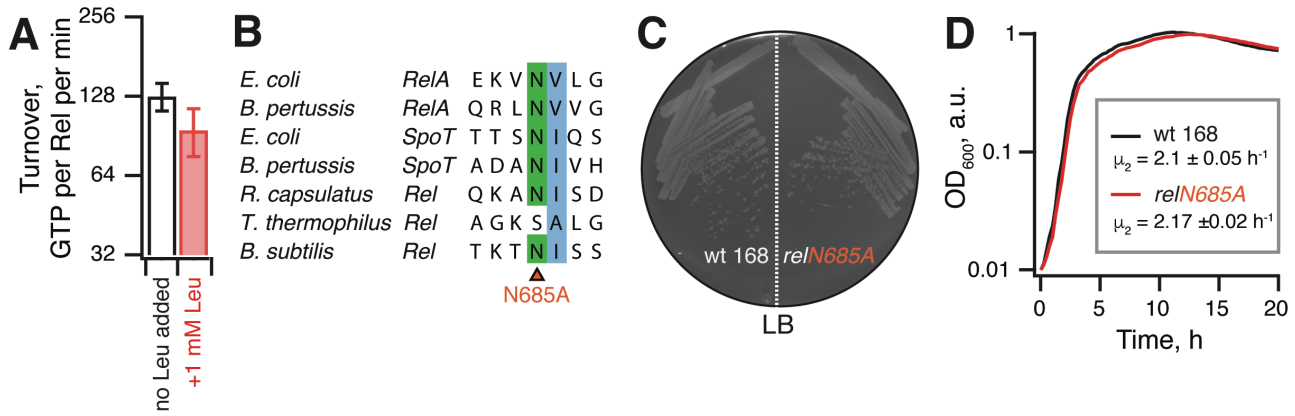

Figure 7. The hydrolysis activity of *B. subtilis* Rel is not activated by branched-chain amino acids binding to the RRM domain. (**A**) Hydrolase activity of *B. subtilis* Rel is not stimulated by leucine. The experiments were performed in HEPES:Polymix buffer, pH 7.5 at 37 °C in the presence of 5 mM Mg^{2+}. Error bars represent standard deviations of the turnover estimates by linear regression using four data points. (**B**) Sequence alignment of the *B. subtilis* N685 region of representative long RSHs. (**C** and **D**) Wild-type *B. subtilis* 168 and isogenic chromosomal *relN685A* mutant (VHB455) were grown on solid (**C**) and liquid (**D**) LB media at 37 °C. The plate was scored after 12 hours at 37 °C. The growth rates (μ^2) were calculated from three independent biological replicates and the error bars (shown as shadows) represent standard deviations. Since the liquid media growth experiments were performed in plates format in Bioscreen C growth curve analysis system the OD_{600} is presented in arbitrary units.